

CARBONATE PETROGRAPHY AND GEOCHEMISTRY
OF THE EISS LIMESTONE OF KANSAS

by 149

PAUL L. DOWLING, JR.

B. S., Old Dominion College, 1965

A MASTER'S THESIS

submitted in partial fulfillment of the
requirements for the degree

MASTER OF SCIENCE

Department of Geology and Geography

KANSAS STATE UNIVERSITY
Manhattan, Kansas

1967

Approved by:

Douglas H. Brooks
Major Professor

LD
2668
T4
1967
D747
C.2

CONTENTS

Introduction.....	1
Purpose of the Investigation.....	1
General Description and Areal Location.....	2
General Facies Variations.....	7
Lithology.....	8
General Discussion.....	8
Lower Limestone Unit.....	11
Middle Shale Unit.....	16
Upper Limestone Unit.....	16
Method of Investigation.....	22
Sampling Procedure.....	22
Laboratory Techniques.....	22
Acid Etching and Staining.....	25
Thin-Sections.....	26
Powdered Sample Preparation.....	26
X-ray Spectrographic Analyses.....	26
Oxide Analyses.....	29
Ferrous Iron and Insoluble Residue Determinations.....	29
Magnesium Analyses by Atomic Absorption.....	34
Clay Mineral Determinations.....	35
Sr ⁸⁷ /Sr ⁸⁶ Initial Ratio Determinations.....	37
Petrography.....	40
General Discussion.....	40
Lower Eiss Limestone Unit.....	55
Upper Eiss Limestone Unit.....	60
Petrographic Environmental Discussion.....	62
Clay Mineralogy.....	67
General Discussion.....	67
Lower Eiss Limestone Unit.....	69
Upper Eiss Limestone Unit.....	72

Calcium and Magnesium Geochemistry.....	73
Aragonite - Calcite Relationships.....	73
Precipitation Mechanism.....	74
The Role of Magnesium.....	75
Calcium/Magnesium Ratios.....	79
Eiss Limestone Ca/Mg Consideration.....	82
Strontium Geochemistry.....	89
Eiss Limestone Sr/Ca Consideration.....	97
Strontium Isotopic Analyses.....	103
Iron and Manganese Geochemistry.....	108
General Discussion.....	108
Eiss Limestone Fe/Mn Considerations.....	115
Silicon Geochemistry.....	123
Bulk Chemistry.....	127
Environment of Deposition.....	132
Discussion.....	132
Conclusions.....	136
Final Conclusion.....	140
Acknowledgments.....	141
Appendix.....	142
References.....	154

FIGURES

Figure 1:	Correlated sections of Eiss Limestone.....	10
Figure 2:	Flow sheet of laboratory procedures.....	24
Figure 3:	Eiss Limestone ferrous iron calibration curve.....	33
Figure 4:	Fossil facies of Eiss Limestone.....	57
Figure 5:	Textural parameters of Eiss Limestone.....	59
Figure 6:	Elias' faunal realms.....	64
Figure 7:	Faunal realms of Eiss Limestone.....	66
Figure 8:	Clay Mineralogy of Eiss Limestone.....	71
Figure 9:	Insoluble residue vs. Ca/Mg ratios for Eiss Limestone.....	85
Figure 10:	Ferrous iron vs. magnesium for Eiss Limestone.....	87
Figure 11:	Magnesium vs. strontium for Eiss Limestone...	99
Figure 12:	Strontium vs. location for Eiss Limestone...	102
Figure 13:	Marine $\text{Sr}^{87}/\text{Sr}^{86}$ geochron.....	106
Figure 14:	Iron stability diagram.....	110
Figure 15:	Manganese stability diagram.....	112
Figure 16:	Ferrous iron vs. ferric iron vs. manganese for Eiss Limestone.....	118
Figure 17:	Manganese vs. calcium for Eiss Limestone....	121
Figure 18:	Insoluble residue vs. silicon for Eiss Limestone.....	125

PLATES

Plate I:	Stratigraphic section of Council Grove Group.....	4
Plate II:	Index map of Eiss Limestone localities.....	6
Plate III:	Tuttle Creek West Dsm Eiss Limestone.....	13
Plate IV:	Deep Creek lower Eiss Limestone.....	15
Plate V:	Tuttle Creek Esst Spillway Eiss Limestone.....	18
Plate VI:	Deep Creek upper Eiss Limestone.....	21
Plate VII:	Paleogeography of the Eiss sea.....	134

TABLES

Table 1:	X-ray spectrograph operating conditions.....	28
Table 2:	Oxide analyses of Eiss Limestone sample 1083...	30
Table 3:	Folk's classification of carbonate rocks.....	42
Table 4:	Textural parameters of lower Eiss Limestone....	48
Table 5:	Fossil parameters of lower Eiss Limestone.....	50
Table 6:	Textural parameters of upper Eiss Limestone....	52
Table 7:	Fossil parameters of upper Eiss Limestone.....	54
Table 8:	Sr/Cs ratios for various carbonate matrices....	91
Table 9:	Average strontium content of various carbonates.....	95
Table 10:	Carbonate $\text{Sr}^{87}/\text{Sr}^{86}$ Analyses.....	107
Table 11:	Oxide analyses of Eiss Limestone.....	129
Table 12:	Chemical relationships in Eiss Limestone.....	131

Dedicated to the memory of the writer's grandparents,
Mr. and Mrs. Andrew Wyper, Sr., whose continued love and
devotion provided nineteen years of educational encouragement
and whose memory will remain an integral part of the writer's
future endeavors.

INTRODUCTION

Purpose of the Investigation

The petrographic study of limestones is complex yet stimulating, but studies based on petrographic considerations alone have been of limited value in discussing problems such as geological correlation, pre- and post-depositional conditions, and related topics.

An attempt has been made in this thesis to use geochemical theory and techniques to resolve some of these limitations, as the writer believes that a combination of both geochemical and petrographic approaches to the study of limestones is warranted.

The Eiss Member of the Bader Limestone Formation was chosen for this study because of the following:

- (1) The lack of previous analytical work on the Eiss.
- (2) The availability of numerous described outcrop locations.
- (3) A minimum stratigraphic thickness for sample control.
- (4) The apparent persistence of like lithologies within each bed but unlike lithologies between beds.
- (5) The lack of post-depositional mineralization and/or alteration.

General Description and Areal Location

The Eiss Limestone is a member of the Bader Limestone Formation which was named by Condra (1927). At first, the Eiss Limestone was included in the Garrison Formation, but later Condra (1935) redefined its units to include the Eiss Limestone as part of the Bader Limestone (Plate I). The type section of the Eiss Limestone (Condra, 1935) is located eight miles south of Humbolt, Nebraska, in the SE 1/4 sec. 3, T. 1 N., R. 13 E. The Eiss Limestone underlies the Hooser Shale and overlies the Stearns Shale in all localities of this investigation.

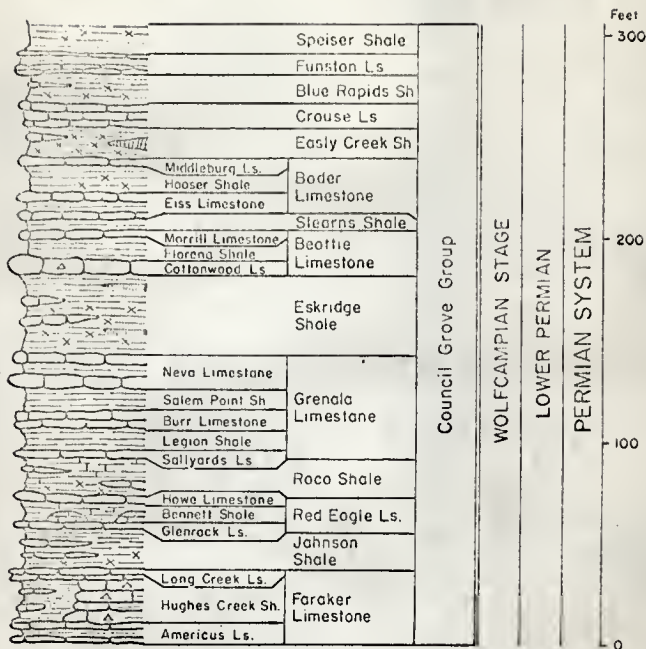
The outcrop area of the Eiss Limestone extends from Humbolt, Nebraska, to the Oklahoma State Line. For this thesis, well exposed sections of the Eiss Limestone were studied in the NW 1/4 SW 1/4 sec. 24, T. 9 S., R. 7 E. of Riley County; in the SW 1/4 NE 1/4 sec. 18, T. 9 S., R. 8 E. of Pottawatomie County; in the NW 1/4 NE 1/4 sec. 29, T. 11 S., R. 8 E. of Geary County; in the SW 1/4 SE 1/4 sec. 13, T. 12 S., R. 10 E. of Wabaunsee County; and in the SE 1/4 sec. 31, T. 18 S., R. 8 E. of Chase County (Plate II).

The Eiss Member consists of two limestones separated by a shale. The upper limestone, 2 to 3 feet thick, is siliceous, porous, and contains local shale breaks. The middle section (2 to 11 feet thick locally) consists of gray fossiliferous, calcareous shale. The lower limestone, 0.5 to 4 feet thick, is characteristically argillaceous, thin-bedded and fossiliferous. Macroscopic fossils found in the two limestones are: Aviculopecten occidentalis,

EXPLANATION OF PLATE I

Stratigraphic section of Council Grove Group, Wolfcampian Stage, Lower Permian Series, Permian System (adapted from Jewett, 1959).

PLATE I

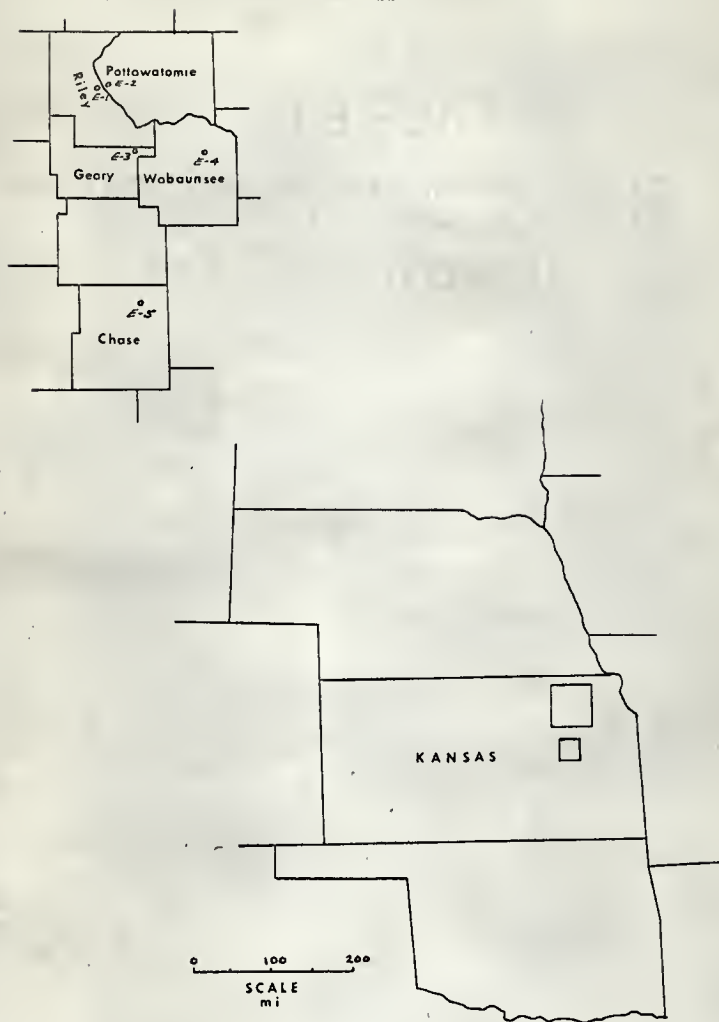


STRATIGRAPHIC SECTION OF COUNCIL GROVE GROUP

EXPLANATION OF PLATE II

Map showing location of samples of Eiss Limestone.

PLATE II



LOCATION OF SAMPLES

Pseudomontis hawni, Myalina, Meekella striatocostata, Derbyia crassa, Composita, Anchicodium and Osagia alga, and a few echinoid spines and crinoid columns. The average thickness of the Eiss Member is about 8.0 feet. The Eiss forms the first prominent hillside bench between the Cottonwood Limestone and Crouse Limestone. The bench is formed by the upper Eiss Limestone only, which weathers to rectangular blocks, one to two feet in diameter. For detailed descriptions, the reader is referred to the measured sections E-1, E-2, E-3, E-4, and E-5 in the appendix.

General Facies Variations

No definite horizontal macro-facies is apparent in the upper Eiss Limestone unit, but the lower Eiss Limestone unit thins locally to the south which might indicate a facies development in that direction. It is difficult to approach the problem of facies change in Kansas Permian limestones, as in the Eiss, since the sporadic movements of the seas over short time intervals created local shorelines with great rapidity.

Several authors (Mudge, 1952, and Mudge and Crumpton, 1959) have tended to break the upper Eiss Limestone unit into two separate limestones in the northern section, but this writer does not agree with their interpretation. The separation only defines local shale partings indicative of the shallow fluctuating conditions which prevailed during the depositional history of the Eiss Limestone Member.

LITHOLOGY

General Discussion

The Eiss Limestone Member ranges in thickness from 10.8 feet at the Allendorph, Kansas, location to 3.3 feet at the Strong City, Kansas, location. A gradual increase in thickness of the entire member was noted from the northern Tuttle Creek location to the Allendorph location with a rapid thinning further south toward Strong City (Fig. 1). The fluctuations in thickness are expressions of the thickening and thinning of the lower limestone and middle shale units. The upper limestone unit remains uniform in thickness throughout the entire outcrop area.

At each location three distinct units of the Eiss Limestone Member were noted. The lower unit in general is an argillaceous fossiliferous limestone which exhibits platy weathering and is in places quite like a calcareous shale. The contact between the lower limestone unit and the middle shale unit is more gradational than abrupt, and in some outcrops a definite lithologic break is absent. Lithologically, only a decrease in calcium carbonate content and slight faunal fluctuations separate the middle shale unit from the lower limestone. The upper limestone unit is a very resistant, siliceous, pitted, fossiliferous limestone which forms a hillside bench at several of the outcrop localities. A definite break in the lithology from the middle shale unit to the upper limestone unit with a sharp contact is characteristic. Several local calcareous shale breaks were noted in the upper limestone

EXPLANATION OF FIGURE 1

Measured sections of Eiss Limestone:

Tuttle Creek West Dam

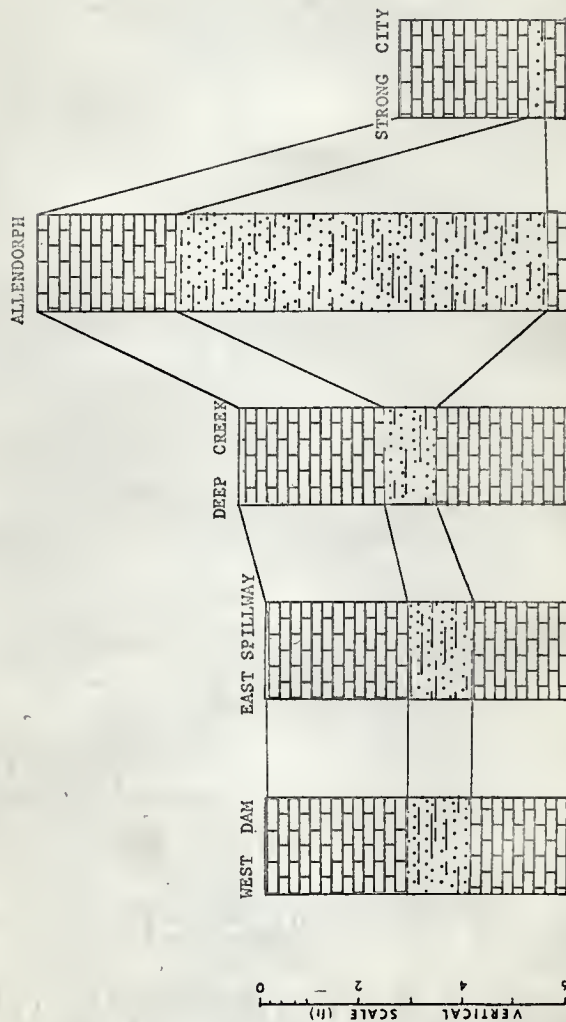
Tuttle Creek East Spillway

Deep Creek

Allendorph

Strong City

FIGURE 1



unit, but these did not warrant the further separation of this limestone into sub-units. Plate III shows a typical exposure of the Eiss Limestone Member at the northern Tuttle Creek West Dam locality.

Lower Limestone Unit

The lower Eiss Limestone unit does not form a distinctive outcrop bench at any of the locations studied. The thickness of the lower unit ranges from 1.8 feet at the Tuttle Creek Dam and Spillway locations to the north to 0.4 feet at the Allendorph and Strong City locations to the south. At the Deep Creek location the lower unit thickens to 2.7 feet. Plate IV shows a characteristic outcrop of the lower Eiss Limestone at the Deep Creek locality.

The color of the lower limestone unit is influenced by the high amount of argillaceous insoluble residue. The unweathered surface is medium gray (N-5) and weathers to a lighter gray (N-7).

The lower Eiss Limestone unit is characteristically more fossiliferous than the upper limestone unit. Gastropods, brachiopods, pelecypods, and bryozoan fragments are found in almost every section. Minor amounts of algae, echinoids and crinoids are present also. The most abundant brachiopods present are Chonetes, Derbyia crassa, and Meekella striatocostata. The pelecypod Aviculopecten occidentalis was noted at several outcrops while other genera of pelecypods exist but were not specifically identified. Rhombopora and Fenestella were the two most abundant bryozoans present and were chiefly located in the northern outcrop

EXPLANATION OF PLATE III

Tuttle Creek West Dam Eiss Limestone. Note typical weathered
outcrop of Eiss Limestone above and below rockhammer.

PLATE III



TUTTLE CREEK WEST DAM EISS LIMESTONE LOCALITY

EXPLANATION OF PLATE IV

Deep Creek lower Eiss Limestone. Note gradational contact between lower limestone and middle (rockhammer) shale.



DEEP CREEK LOWER EISS LIMESTONE LOCALITY

areas. The gastropods represent the small (2mm x 1mm), high-spired variety. Positive identification of the gastropods was not possible, but they do resemble Holopea sp. reported by Mudge and Yochelson (1962).

Middle Shale Unit

The middle shale unit was not investigated in this thesis due to the emphasis on carbonate geochemical correlation. Lane (1964) and Dietsch (1956) have previously studied the middle shale unit. The variations in thickness of the middle shale unit appear to be the controlling factor in the total thickness of the Eiss Limestone Member.

Upper Limestone Unit

The upper limestone unit is the thickest and most consistent limestone in the Eiss. The thinnest section of the upper limestone unit occurs at Strong City where it is 3.2 feet thick, while it reaches a maximum thickness at the Tuttle Creek Dam and Spillway locations where it is 3.8 feet thick. Due to the areal consistency of the thickness, no stratigraphic trend was noted in the upper as was in the lower limestone unit. The upper limestone unit at all localities forms a definite hillside bench. In fact, this bench is the most prominent limestone bench immediately above the Cottonwood Limestone (Plate V). In fresh outcrops, the

EXPLANATION OF PLATE V

Tuttle Creek East Spillway Eiss Limestone. Note bench forming
characteristic of upper limestone.



TUTTLE CREEK EAST SPILLWAY EISS LIMESTONE LOCALITY

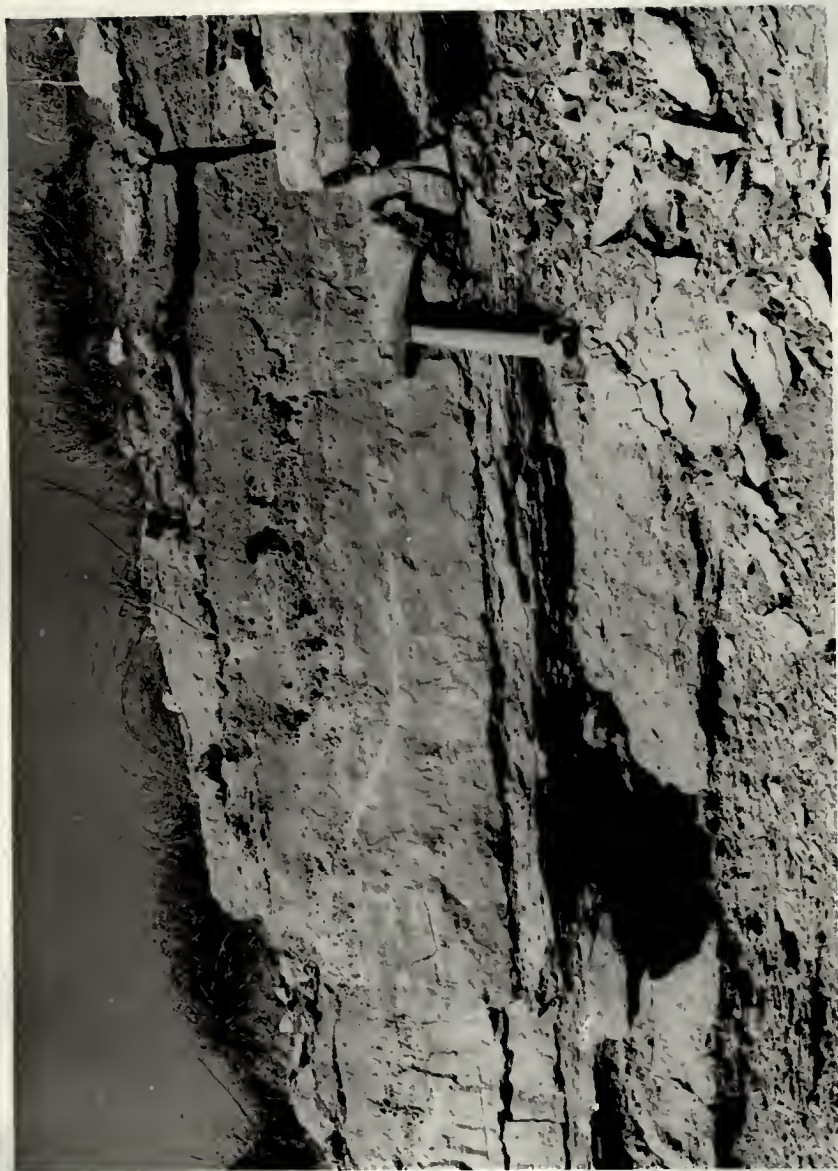
upper limestone unit is quite massive and blocky; but upon weathering becomes pitted with solution cavities (Plate VI).

The upper limestone unit is less argillaceous and therefore contains less insoluble residue than the lower limestone unit, but it does contain definite local shale breaks (Plate VI). The upper limestone unit does not have a gradational but a sharp contact with the underlying middle shale unit and the overlying Hooser Shale.

Fossils in the upper limestone unit are quite similar to those in the lower limestone unit. There does appear to be an increase in the number of pelecypods and algae, but gastropods and brachiopods remain relatively constant in number. Aviculopecten occidentalis, Pseudomontis hawni, and Myalina are the dominant pelecypods while brachiopods are represented by Meekella striacostata and Derbyia crassa. Algae is predominantly Anchicodium with some Osagia present.

EXPLANATION OF PLATE VI

Deep Creek upper Eiss Limestone. Note shale breaks and solutioned surface characteristic of the Eiss Limestone in several localities.



DEEP CREEK UPPER EISS LIMESTONE LOCALITY

METHOD OF INVESTIGATION

Sampling Procedure

Field samples were collected at measured outcrop sections of the Eiss Limestone Member (Fig. 1). In order that contamination be kept at a minimum, surface material was removed to a depth of four inches before the actual samples were taken. The selection of sample sites within the individual measured sections depended upon the following:

- (1) Characteristic lithologic changes within the Eiss limestone both vertically and horizontally.
- (2) Sampling at approximately the same horizon in some sections for correlation purposes, while in others channel samples were taken to obtain an average sample.
- (3) Avoidance of local concentrations of post-deositionally altered zones.

Samples were logged, stored in sand sample bags, and returned to the laboratory for further examination.

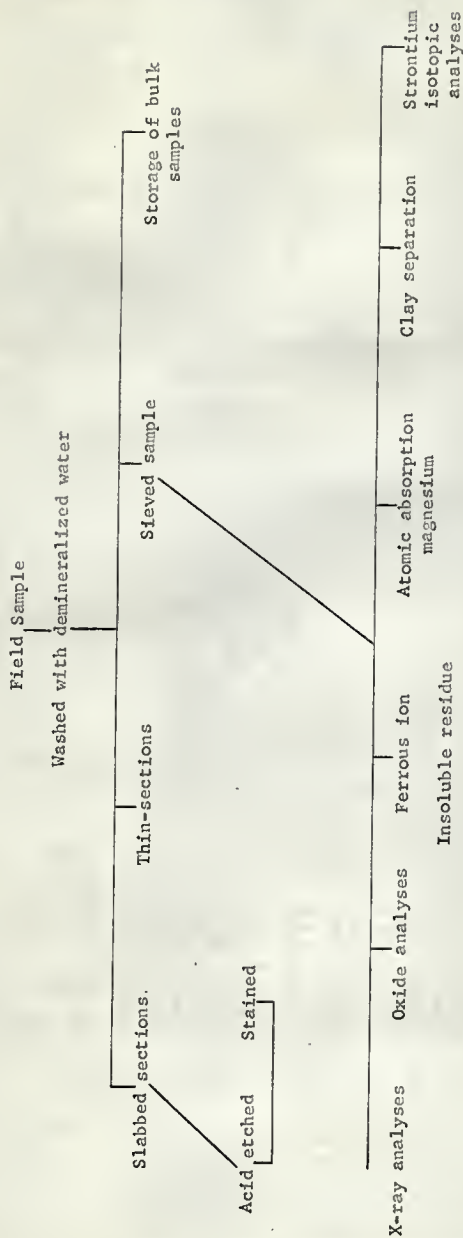
Laboratory Techniques

To facilitate a minimum of repetition in description of the laboratory procedures a flow-sheet was made (Fig. 2). Prior to any laboratory investigation the field samples were cleaned and rinsed with demineralized water.

EXPLANATION OF FIGURE 2

Flow sheet of laboratory procedures used to facilitate rapidity and reproducibility in all research techniques.

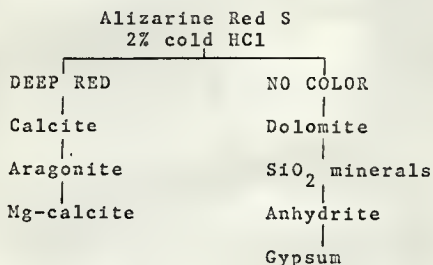
FIGURE 2



FLOW SHEET OF LABORATORY PROCEDURES

Acid Etching and Staining

A representative slab of each field sample was cut and polished with #100 corundum grit. After polishing, the slab was etched in 0.5 normal hydrochloric acid for approximately three minutes. The acid dissolved the calcite, aragonite, and Mg-calcite and left the dolomite and non-carbonate fractions clearly exposed on the slab surface. Staining of the etched slab was done according to the method of Friedman (1959). A 0.1 gm alizarine red S per 100 cc 0.2% cold hydrochloric acid solution was made and applied to the etched slab for two to three minutes. The expected results of this method are shown below:



Further staining techniques would have differentiated between pairs (i.e. dolomite - anhydrite), but for the purpose of this investigation only the gross percentages of calcite and dolomite were required. The above technique works quite well with limestone consisting of dolospar or patches of dolomicrospar or dolomicrite. For the Eiss Limestone, however, all X-ray diffraction dolomite values were low and occurred in the form of minute clusters of dolomicrite; therefore, limiting the applicability of the alizarine red S staining technique. All samples exhibited

degrees of silica replacement of fossils and horizontal trends of clay mineral floods, but no definite calcite-dolomite percentages could be obtained from the method.

Thin-Sections

All thin-sections were prepared commercially from cut-slabs. The results of the thin-section petrography will be discussed later.

Powdered Sample Preparation

A representative slab from each sample was chosen for powder preparation. The slab was crushed in a steel mortar and pestle then sieved to a -200 mesh grain size. After sieving, each sample (approximately 200 grams) was stored in individual glass bottles. To avoid contamination from the previous sample, all equipment was washed with 2.0 normal hydrochloric acid after being used. In addition, the first aliquot of the next sample was discarded then the remaining sample collected. Thus the error in sample preparation was controlled for all future analyses.

X-ray Spectrographic Analyses

All powdered samples were examined by X-ray spectrography to obtain the percentages of Ca^{++} , Sr^{++} , Si^{++} , total Fe, and Mn. Analyses for Mg were attempted but it was found that the mylar window in the sample holder cut down the detectability of Mg

by a factor of 10. Since the Mg values were so low, the use of X-ray spectrography would have been impossible.

A Norelco X-ray spectrograph was used for each analysis. In Table 1 are outlined the operating conditions for each element detected by the X-ray spectrographic method.

After coning and quartering, each sample was analyzed at least in duplicate being repacked each run in the sample holder. After all of the Eiss samples and the Kansas State University laboratory limestone standard AB_4 had been analyzed in duplicate, the percentages of elements were determined for the unknowns. The percentage of an unknown element is proportional to its peak height (i.e. difference in counts per second between background and peak height) and each peak height can be compared to the peak height of the same element in a standard (AB_4). It is the personal opinion of the writer that a $\pm 5\%$ value probably represents a minimum for the Norelco equipment. Although values for an error of less than 1% have been reported using this equipment, only with several standards of the same matrix as the unknown and numerous repetitive analyses can one obtain very accurate results. Included in the $\pm 5\%$ error of the analyses are the following:

- (1) Incomplete mixing of the standard or the unknown.
- (2) Fluctuation in machine stability or settings.
- (3) Possible contamination of standard or unknown.
- (4) Sample packing inconsistencies.
- (5) Error in the original commercial oxide standard analysis (AB_4).

Table 1

X-ray Spectrograph Optimum Operating
Conditions for Cation Analyses

Element	Tube	Crystal	kV	ma	Detector Voltage	L	W	Peak Used
Ca	Cr	Pet	50	28	1.56	5	7	k β .
Sr	Mo	Topaz	50	50	0.88	6	6	k α .
Si	CR	Pet	50	28	1.64	10	14	k α .
Total Fe	Mo	Topaz	50	50	0.98	6	10	k α .
Mn	CR	Pet	50	28	1.56	17	6	k α .

Oxide Analyses

A commercial oxide analysis was made from the Permian Eiss Limestone unit at the East Spillway locality (sample number 1083). Table 2 lists the results of the oxide analysis.

Although no error was reported in the correspondence with the commercial analyst, Smith (1967) has shown that several of his analyses were inaccurate (performed by the same personnel). Because of this fact the writer believes the \pm 5% error in the Eiss X-ray analyses is not too significant.

Ferrous Iron and Insoluble Residue Determinations

Ferrous iron and insoluble residue analyses were performed on the same sample aliquot. Ferrous iron was determined using a modified method described by Lanning (1965). Five grams of each sample were placed in a 600 ml. beaker. The beakers were heated four hours at 115° C to drive off moisture, and then equilibrated for one hour at room temperature. After equilibration 50 ml. of 6.0 normal hydrochloric acid were added to each sample and the resulting solution boiled for thirty minutes. The strength of the acid combined with the boiling will produce a digested sample which contains all available ferrous ions, including that leached from the insoluble material. After digestion the samples were filtered and the beaker washed with 50 ml. demineralized water. Upon filtration, the insolubles were washed and then stored for future insoluble residue determination. Two hundred ml. demineralized water and 10 ml. concentrated phosphoric acid were

Table 2

Commercial Oxide Analysis of
Eiss Limestone Sample 1083

Results of Chemical Analysis

	Eiss <u>1083</u>
SiO ₂	6.46
Al ₂ O ₃	1.23
Fe ₂ O ₃	0.21
FeO	0.24
MgO	0.78
CaO	50.21
Na ₂ O	0.06
K ₂ O	0.25
H ₂ O(+)	0.52
H ₂ O(-)	0.27
TiO ₂	0.05
MnO	0.03
P ₂ O ₅	0.03
CO ₂	39.28
SO ₃	0.08
SrO	0.014

then added to the filtrate. The solutions were well stirred. Just prior to titration, two drops of Ferroin indicator were added to each beaker. Each sample was then titrated from red to blue with ceric ammonium sulfate solution. The actual ferrous ion percentage obtained is given by the following equation:

$$\frac{(\text{ml to titrate sample}) \times (0.01) \text{ gms Fe}^{\text{II}}/\text{ml}}{\frac{\text{ml to titrate standard}}{\text{wt. of sample in grams}}} \times 100 = \% \text{ Fe}^{\text{II}}$$

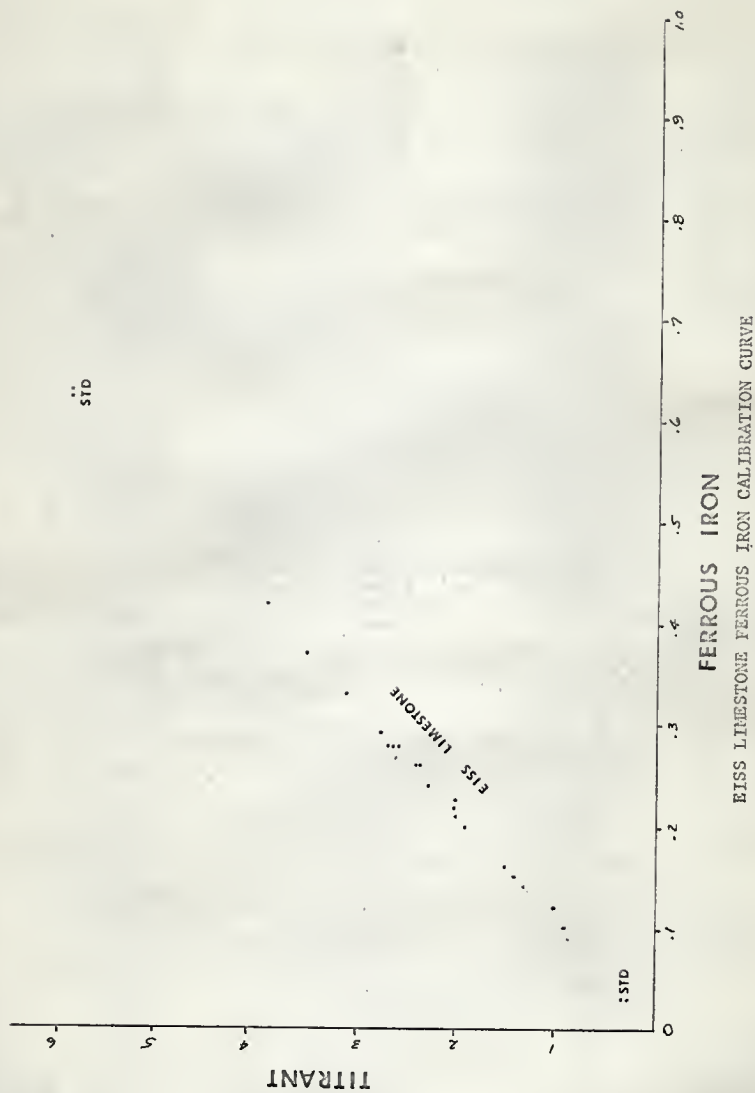
The original analyses of Kansas Permian limestones (Lanning, 1965) called for employing a nitrogen atmosphere during the ferrous iron analyses. The writer found that this method was unsatisfactory due to inconvenience of apparatus construction and the large volume of nitrogen necessary for each analysis. Therefore, in all ferrous analyses, the writer used an air atmosphere. After plotting ml of titrant against weight per cent of ferrous iron (Fig. 3) the resulting comparison shows that no apparent oxidation of the ferrous ion takes place in an air atmosphere. All samples were analyzed in duplicate and an average ferrous ion value obtained.

The insoluble material remaining after the ferrous filtration was weighed to 0.0001 gram and the percentage insoluble residue calculated on the basis of the original 5 gram samples. In order not to lose any insoluble material, the insolubles plus the filter paper were weighed and the weight of the filter paper accounted for.

EXPLANATION OF FIGURE 3

Calibration curve of Eiss Limestone and laboratory standard ferrous iron samples. No apparent oxidation of ferrous to ferric iron occurred as evidenced by the straight line relationship of all samples and standards.

FIGURE 3



The error involved in the ferrous ion determination is approximately $\pm 2\%$ and that of the insoluble residue analyses even less. The apparent error in the ferrous analyses is a result of laboratory technique and contamination, rather than procedural error or oxidation.

Magnesium Analyses by Atomic Absorption

A 0.1 gram aliquot of each sample was weighed and digested in 2 normal hydrochloric acid for two hours. Complete dissolution was not attained, but sufficient dissolution was attained so that all magnesium was leached from the insolubles.

The samples were then filtered and washed with demineralized water into 200 ml flasks. A 20 ml lithium 0 standard solution was added and all solutions were diluted to 200 ml with demineralized water. The lithium 0 standard solution was added for possible future flame photometric analyses.

Standard magnesium solutions were prepared in the same manner except that no dissolution was required. The standard solutions were calibrated in magnesium ppm of values 0 ppm Mg, 2.5 ppm Mg, 5 ppm Mg, 20 ppm Mg, 40 ppm Mg, 60 ppm Mg, 80 ppm Mg, and 100 ppm Mg. Although only the 0 to 20 ppm Mg standards fall in the range of all unknown Eiss analyses, the remaining Mg standards were used to calibrate the atomic absorption apparatus and to prepare the absorption curve of magnesium.

A Jarrel-Ash atomic absorption unit was used combined with a Sargent chart recorder. An air/C₂H₂ fuel ratio of $\frac{27.5 \text{ l/min.}}{42 \text{ l/min.}}$

was found to be satisfactory for the magnesium 2852 Å absorption line. An RCA - IP28 photomultiplier tube at 540 volts and a Jarrel-Ash hollow cathode magnesium source at 15 milliamps combined with a one-half meter grating satisfied the detectibility requirements for this element. Using the atomic absorption apparatus, a sensitivity minimum of 0.01 ppm magnesium could have been obtained; but valves with an error of ± 2 ppm magnesium were found to be satisfactory. The calibration curves for the magnesium standards and unknowns show the accuracy of this method. All samples were analyzed only once since the sample feed permitted a long scan of the magnesium line and therefore increased the measured stability. Deionized water was introduced into the apparatus after each unknown in order to clean the burner as well as produce a zero magnesium line.

Of all the analytical techniques used in the laboratory, with the exception of $\text{Sr}^{87}/\text{Sr}^{86}$ initial ratio analyses, the atomic absorption technique was found to be the most accurate and reproducible.

Clay Mineral Determinations

Approximately 10 grams of each sample were digested in 0.2 normal acetic acid until all the carbonates had been removed. The resulting insolubles, therefore, would be free of the carbonates, yet no stray clay mineral alteration should occur due to the low normality of the acid. Subsequent X-ray diffraction scans

showed that some of the original calcite structure remained, indicating a minimum leaching effect on the insolubles.

After dissolution all samples were filtered with deionized water. Since the percentage insoluble residue had been previously calculated, accurate weighing procedures were not followed in the clay separation.

Following filtration all samples were transferred from the filter paper to 600 ml beakers. Four hundred milliliters of deionized water were then added and the solution was immediately stirred. After several minutes a few of the samples began to flocculate and 1.5 grams of commercial Calgon detergent (sodium hexametaphosphate) were immediately added and the sample restirred. With the addition of several more grams of Calgon it was found that all the samples had deflocculated. At this time the samples were again stirred and left for eight hours. After eight hours 4 ml of the clays which remained in solution were removed by pipette and placed on glass petrographic slides. The slides were allowed to dry overnight, which facilitates the orientation of the clay minerals.

After drying the clay mineral identifications were determined by the use of a Norelco X-ray diffractometer. A Cu target was used at KV 38 and MA 18 settings with L=7, W=6 and a detector voltage of 1.70 volts. Full scan patterns were obtained in the range of 0 to 50 degrees 2 θ .

Since certain clay minerals expand upon the addition of organic compounds to their structure, ethylene glycol was sprayed on each slide to further the identification (of such clays as

montmorillonite). After being sprayed, the slides were again run between 0° - 15° 2θ . In this range expansion will show up most accurately.

Only the oriented and glycolated treatments were used with the clay minerals since the writer was interested only in a qualitative analysis of the clay mineral fraction of the Eiss Limestone.

Both the insoluble material and the remaining clay fraction were stored in labeled glass sample bottles containing deionized water. This procedure was used since clays or small grain size insolubles are almost impossible to put into solution after they have dried.

$\text{Sr}^{87}/\text{Sr}^{86}$ Initial Ratio Determinations

Due to the constant threat of contamination in any isotopic procedure, all isotopic laboratory techniques were carefully monitored to avoid contamination. The procedure used for the preparation of carbonates for strontium isotopic analyses are those of the Kansas State University Geochronology Laboratory. In order to minimize future error the procedure is outlined as follows:

- (1) Wash off any surficial dirt and rinse with demineralized water; dry.
- (2) Grind in an agate mortar and sieve; collect the minus 200 mesh fraction.

- (3) Dissolve about 0.5 grams in 15 ml of vycor distilled 2 normal hydrochloric acid (this step takes about twenty minutes with occasional stirring).
- (4) Add enough Sr^{85} tracer to produce 0.4 to 0.5 mR/hr activity.
- (5) Filter through No. 576 (Schleicher and Schuel) paper until all activity is in the filtrate.
- (6) If the volume of filtrate is greater than 25 ml, evaporate volume down to 10 ml and refilter.
- (7) Carefully pour filtrate on a clean ion exchange column being careful not to disturb the resin top; wash the column sides down with 2 normal hydrochloric acid. Use a minimum of acid.
- (8) After the filtrate has soaked into the resin, carefully add about 20 ml acid, repeat two or three times until the Sr^{85} activity is at least one inch below the resin surface.
- (9) Add 2 normal hydrochloric acid until the activity is about one-half inch above the quartz wool in the bottom of the column; this step takes anywhere from 450 to 600 ml acid.
- (10) Collect in 20 ml aliquots in a polypropylene beaker until all activity has passed through the column.
- (11) Evaporate the beaker down to 5-10 ml volume.
- (12) Combine beakers showing pronounced activity into a teflon evaporating dish. CAUTION: if the first beaker

showing activity reads less than 0.05 mR/hr. calcium may be present in abundance. Evaporate this aliquot separately and inspect precipitate. If large, discard; if very small, combine with other strontium fractions.

- (13) Dissolve residue to about 10 ml in 2 normal hydrochloric acid and repeat steps 5 through 12. This is important since the second run through the column insures against the presence of calcium. Repeat a third time if necessary.
- (14) To the final residue add a few drops of vycor distilled nitric acid and transfer the contents to a 5 ml vycor beaker.
- (15) Evaporate slowly to dryness.
- (16) Carefully fire the residue to red heat over a Meeker burner without spattering. This burns off any resin present and oxidizes the strontium salt(s).
- (17) Cool, seal, label, and store for mass spectrometer analysis.

All mass spectrometer analyses were performed at the Kansas State University Geochronology Laboratory.

PETROGRAPHY

General Discussion

Most limestones are essentially monomineralic, yet their minor constituents and individual different chemistries indicate wide variation in conditions both during and after formation. Previous attempts at classification have involved grain size (Grabau, 1904), texture (Archie, 1952), calcium-magnesium ratios (Chillingar, 1957) and more recently again texture (Folk, 1959). The varying approaches to limestone classification have led to a wide number of names for different types of limestone which can tend to confuse the carbonate petrographer.

For this reason, the classification according to Folk (1959) is used in this thesis, with a few additions by the writer (Table 3). Folk's classification is basically descriptive but does have significant genetic implications. Folk's classification consists of three end-member "poles". These include (1) terrigenous constituents, (2) allochemical constituents, and (3) orthochemical constituents. Each "pole" is defined as follows:

Terrigenous Constituents. Material that has originated outside the basin of deposition and has been introduced into the basin in solid form can be classified as terrigenous. Detrital quartz, feldspar and clay particles are the most common terrigenous constituents.

Allochemical Constituents. Any material that has originated within the basin of deposition, regardless of transport distance,

TABLE 3

Names and symbols in the body of the table refer
to limestones.
Specify crystal size.

can be classified as allochemical. Folk defines four types of "allochems": oolites, fossils, pellets, and intraclasts. The first three types of allochems are in common usage but the term intraclasts requires some explanation. Folk (1959, p.4) genetically defined the term "intraclast" as

"fragments of penecontemporaneous, usually weakly consolidated, carbonate sediment that have been eroded from adjoining parts of the sea bottom and redeposited to form a new sediment."

Physically, intraclasts may be defined as generally ovoid to well-rounded particles composed of microcrystalline calcite which commonly show internal structure. The internal structure may be composed of silt or sand size grains, fossil fragments, smaller intraclasts, oolites or a combination of any of these. Pellets (faecal pellets) are quite similar to intraclasts and in many cases a clear differentiation between the two cannot be made. Illing (1954) defined faecal pellets in the Bahama Banks as friable to well-cemented ellipsoids with a long diameter usually between 0.5 and 0.7 mm, and a ratio between maximum and minimum diameters of about 2.0 mm. Illing's faecal pellets are certainly intraclasts according to Folk's classification, for they are too large to be pellets (0.04 to 0.08 mm), yet their origin is completely different. For this reason, in the descriptive petrology of the Eiss Limestone, pellets and intraclasts will be considered identical in most instances and included in the mollusc count.

.Orthochemical Constituents. Chemical or biochemical precipitates, "allochems", are formed within the basin of deposition and exhibit relatively no evidence of transportation.

In this category Folk includes microcrystalline calcite, sparry calcite, recrystallized calcite, and replacement or authigenic minerals.

Microcrystalline Calcite. Calcite in the grain size range of 1-4 microns in diameter Folk has defined as "micrite". In thin section the grains are equant and irregularly rounded exhibiting a faint brown color under plane polarized light. Calcite of this type is considered to be an ooze formed by rapid chemical or biochemical precipitation followed by immediate settling to the bottom.

Sparry Calcite. Calcite in the grain size range of 10 microns or larger in diameter is defined as "spar". Spar can be distinguished from micrite by its larger grain size as well as crystal clarity. It is obvious that the crystal clarity of spar is directly a function of grain size alone. Sparry calcite forms mainly as a pore-filling cement.

Recrystallized Calcite. Calcite in the grain size range of 5 to 15 microns in diameter is defined by Folk as recrystallized calcite or "microspar". In most cases it has been found to be recrystallized micrite, although spar can undergo the same phenomena. The differentiation between spar and microspar can be very difficult without adequate criteria for distinguishing the two. Stauffer (1962) suggested the following criteria for the recognition of sparry calcite versus recrystallized calcite:

"Criteria directly indicative of sparry calcite:

1. Crystals in contact with a once free surface, such as oolites or the inside of shell chambers.

2. Crystals in the upper part of a former cavity which was partly filled with more or less flat-topped detrital sediment.
 3. An increase in crystal size away from the wall of an allochem.
 4. A decrease in the number of crystals away from the wall of an allochem.
 5. Preferred orientation of the optic axis of crystals normal to the wall of an allochem.
 6. Preferred orientation of the longest diameter normal to the wall of an allochem.
 7. Plane boundaries between crystals.
- Criteria suggestive of sparry calcite:
8. Three dimensional packing of allochems.
 9. Well sorted allochems.
 10. Rounded allochems.
 11. Presence of abundant oolites.
 12. Size of crystals generally larger than 10 microns.
 13. Clear, inclusion free crystals.
 14. Sharp contact between the crystal mosaic and the wall of an allochem.
 15. A crystal mosaic entirely filling a more or less obvious cavity or, if only partly filling it, leaving an empty cavity or space in the center bounded by protruding crystal faces.
- Criteria directly indicative of recrystallized calcite:
1. Irregular grain size of a crystal mosaic with no systematic variation.
 2. Truncation by crystal mosaic or previously existing structures such as laminae of oolites and fossil structures.
 3. Truncation of allochems in crystal mosaic.
 4. Embayments by calcite crystals, which may have plane sides, into microcrystalline calcite of allochems.
 5. Curved, serrated, or interlocking intergranular boundaries between crystals.
- Criteria suggestive of recrystallized calcite:
6. Loosely packed allochems.
 7. Poorly sorted allochems.
 8. Angular allochems.
 9. Gradational boundary between calcite mosaic and microcrystalline calcite.
 10. Calcite crystal size never smaller than four microns and generally larger than seven microns.
 11. Irregular patches of crystal mosaic in microcrystalline calcite.
 12. Residual, irregular, floating patches of microcrystalline calcite in the midst of a coarser calcite mosaic."

According to Folk's classification (1962) the various limestone names are formed from a combination of the previously described constituent names and their relative abundances. Several prefixes added to the basic name distinguish the characteristic terrigenous and fossil material while different suffixes differentiate allochemical grain size.

The Eiss Limestone Member was classified according to the methods of Folk (Table 3). The limestone names and percentages of constituents are shown in Tables 4-7.

For the purpose of facies differentiation the detailed petrographic fossil tabulations were combined into four composite facies:

- (1) Algal bryozoan facies. Rocks of this facies are characterized by grains coated with the algae Osagia. Bryozoans are significantly present with a smaller representation of molluscs, brachiopods and pelecypods.
- (2) Algal shelly facies. This facies is characterized by a high percentage of algae (either Osagia or Anchicodium). Molluscs, brachiopods, and pelecypods are more common here than in the algal bryozoan facies.
- (3) Shelly algal facies. Rocks of this facies are dominantly composed of molluscs, brachiopods, and pelecypods with some algae. Bryozoans are present in very few numbers.

TABLE 4

Textural parameters of Lower Eiss Limestone.

Table 4

Lower Eiss Limestone Unit

Rock Name (Folk)	Unit	Location	Slide	Micrite	Microspar	Spar	Spar Size
Slightly recrystallized bryozoan <u>Osagia</u> biomicrite	upper	West Dam	E1AU	39	13	2	0.21mm
Slightly recrystallized bryozoan <u>Osagia</u> biomicrite	upper	East Spill.	E2B	35	6	6	1.35mm
<u>Osagia</u> molluscan biomicrosparite	upper	Deep Creek	ED-4	21	36	3	0.46mm
Molluscan biomicrosparite	upper	Allendorph	E4A	20	45	1	0.30mm
Echinoderm molluscan biomicrosparite	upper	Strong City	SC-2	18	66	2	0.46mm
Quartz silty recrystallized shelly biomicrite	lower	West Dam	E1AL	28	36	4	0.40mm
Quartz silty recrystallized shelly biomicrite	lower	East Spill	E2A	30	22	9	0.46mm

TABLE 5

Fossil parameters of Lower Eiss Limestone.

Table 5

Lower Eiss Limestone Fauna

Slide	Fossils ²	Brachiopod	Pelecypod	Gastropod	Bryozoa	Algae ¹	Crinoid	Echinoid	Ostracod	Forams
E1AU	46	6	2		14	6	2	4	2	1
E2B	53	2	1	1	19	18		9	1	1
ED-4	40	4	3	15	3	10	1	1	1	1
E4A	34	5	2	9	r			2	3	
SC-2	14	2	2	2			4	3	1	
E1AL	29	6	1	10		5		3	3	1
E2A	36	8	2	19		2		1	1	

¹ All algae Osagia except a trace of Anchiodium.

² Percentage of fossils could be fragmental thanatocoenosis assemblage, (high echinoid, ostracod content could be thanatocoenosis).

TABLE 6

Textural parameters of upper Miss Limestone.

Table 6

Upper Eiss Limestone Unit

Rock Name (Folk)	Unit	Location	Slide	Micrite	Microspar	Spar	Spar Size
Sparry algal biomicrosparite	upper	West Dam	E1BU	30	44	10	0.89mm
Algal microsparite	upper	Spillway	E2D	18	62	3	0.40mm
Algal microsparite	upper	Deep Creek	ED-1	5	61	2	0.25mm
Sparry molluscan microsparite	upper	Allendorph	E4E	9	32	31	1.15mm
Algal dismicrite	upper	Strong City	SC-1	58	T	20	1.40mm
Recrystallized brachiopod biomicrite	middle	West Dam	E1BM	32	28	8	0.46mm
Recrystallized molluscan dismicrite	middle	Spillway	E4D	14	37	31	1.45mm
Algal shelly microsparite	middle	Deep Creek	ED-2	17	66	1	0.25mm
Recrystallized biotismicrite	middle	Allendorph	E4C	20	58	10	0.98mm
Brachiopod microsparite	lower	West Dam	E1BL	25	67	6	0.40mm
Recrystallized brachiopod biomicrite	lower	Spillway	E2C	37	36	2	0.10mm
Shelly biomicrosparite	lower	Deep Creek	ED-3	34	47	5	0.92mm
Recrystallized molluscan dismicrite	lower	Allendorph	E4B	21	39	32	2.70mm

TABLE 7

Fossil parameters of Upper Eiss Limestone.

Table 7

Upper Eiss Limestone Fauna

Slide	Fossils	Brachiopod	Pelecypod	Gastropod	Bryozoa	Algae	Crinoid	Echinoid	Ostracod	Forams
E1BU	16	1	2	2		8			1	
E2D	17	1	2			13			1	
ED-1	32					29			2	
E4E	28	2	5	11		3	1	1	3	
SC-1	22	1				20*			1	
E1BM	32	18	3	4		2		2	1	
E4D	18	1	5	10					2	
ED-2	17	5	3	1		3	1	1	2	
E4C	12	2	2	2		2		1	1	1
E1BL	2	2	T					T	T	
E2C	25	11	1	2		3		T	T	
ED-3	14	3	3	2		2	1	2	1	
E4B	8	2	1	5						

*All algae probably Anchicodium except SC-1 which is Cryptozoon kansasensis.

- (4) Shelly facies. This facies is dominated by the shelly forms - molluscs, brachiopods, and pelecypods. Algae is essentially absent from this population. A high insoluble residue content is generally characteristic of this facies.

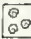
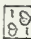


Microphotographs of the significant Eiss Limestone facies are found in the appendix.

Lower Eiss Limestone Unit

Two lateral facies are dominant in the lower Eiss Limestone. The northern localities are algal bryozoan and shelly algal facies while at the Allendorph locality the suite becomes quite shelly with little or no algae (Fig. 4). The shelly facies is also dominant in the extreme southerly Strong City locality. The insoluble residue content (Fig. 5) exhibits an inverse relation to the algal population and a direct relation to the shelly fauna. In the northern Dam and Spillway localities the insoluble content is relatively high but containing a large amount of quartz silt as well as clays. At the latter location, although essentially algal, a shelly fauna exists in one-half of the total population. With a marked decrease in the insoluble content at the Deep Creek locality an absence of the shelly fauna was noted with an increase in algal content. Further south at the Allendorph and Strong City locations the population is all shelly with no algae. The insoluble content at Allendorph is high again and therefore has excluded algae from the biotope. Although the insoluble content is lower

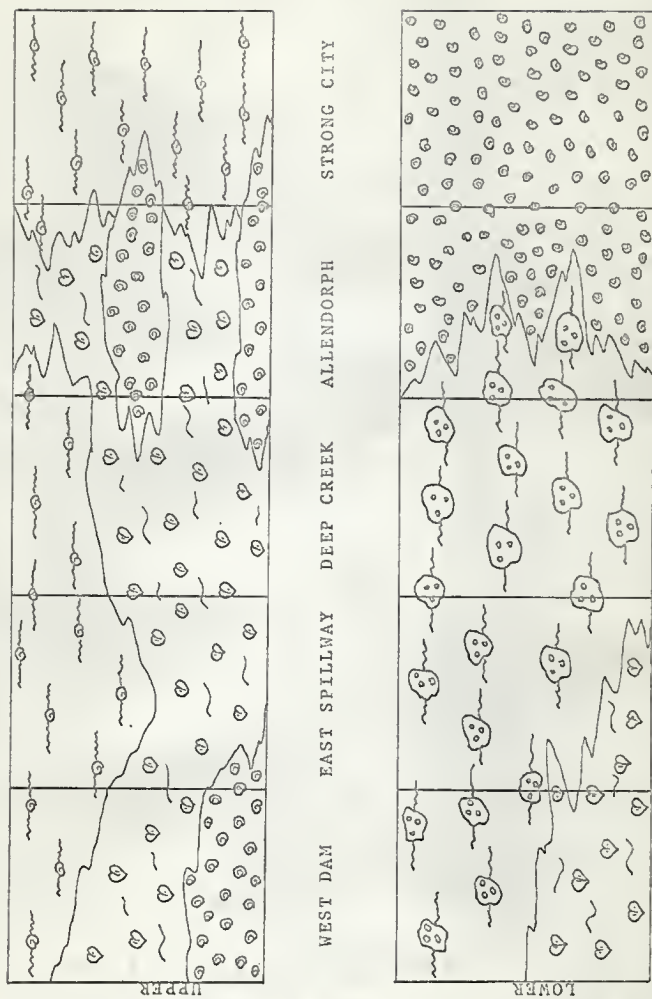
EXPLANATION OF FIGURE 4

Fossil facies of the Eiss Limestone.

-  Shelly facies
-  Shelly algal facies
-  Algal shelly facies
-  Algal bryozoan facies

Each locality is represented by the approximate volume of the facies present.

FIGURE 4

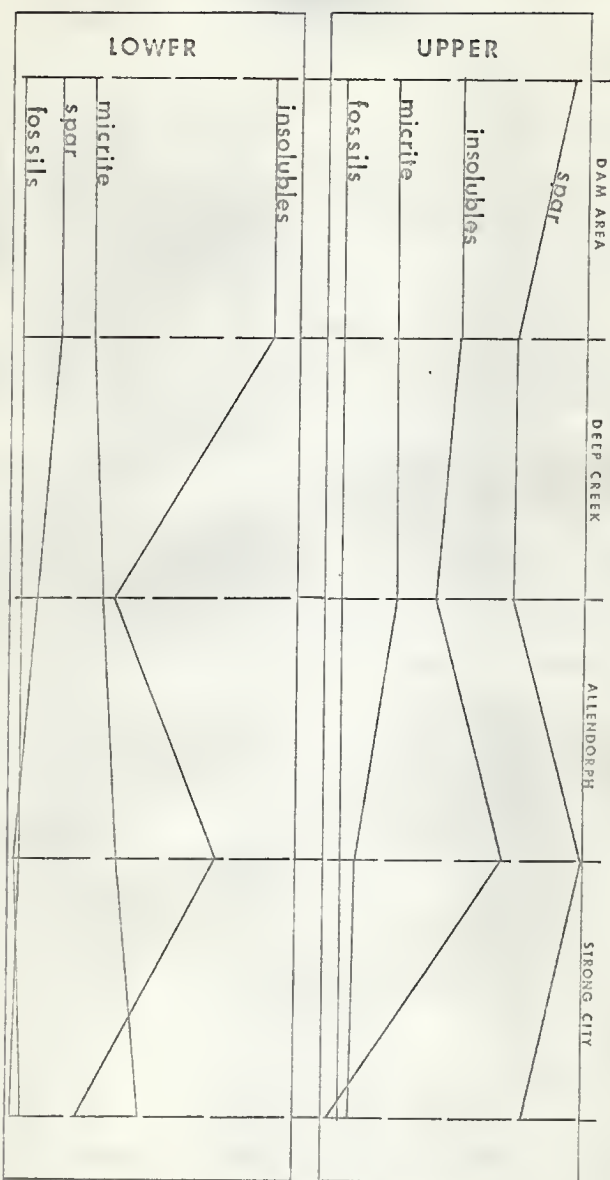


FOSSIL FACIES OF THE EISS LIMESTONE

EXPLANATION OF FIGURE 5

A summary of the textural parameters of the Eiss Limestone at each locality. No vertical scale is used but relative increases and decreases at each locality can be noted. Micrite and microspar are totaled as both are considered to be or have been carbonate mud.

FIGURE 5



TEXTURAL PARAMETERS SUMMARY OF THE FISS LIMESTONE

at the Strong City locality, the increase is micrite and microspar appear to control the fauna and not the insolubles. The greater amount of carbonate mud at this locality could have created restricted bottom conditions which are evidenced by not only the absence of algae but a decrease in total faunal content.

The algal-shelly facies to the north could indicate a shallower environment with rapid influx of terrigenous material from a nearby northern lowland source. The shelly facies to the north is considered to be either a deeper portion of the Eiss seas or a different chemical environment which would exclude the algal-bryozoan population. If the water were deeper the facies could be interpreted as that of normal salinity and quieter water below the zone of maximum turbulence. The increase of micrite and microspar would be indicative of the latter environment. But if the pH of the system had changed in such a way as to further the increased precipitation of carbonates the change could have restricted the fauna to the more hardy shelly types.

Upper Eiss Limestone Unit

Lateral and vertical faunal variations occur within the upper Eiss Limestone (Fig. 4). The northern localities are mixed algal and shelly algal while at the Allendorph locality the population becomes less algal and more shelly. In the southern area at Strong City the population is almost 100 per cent algal. The insoluble content is relatively constant in the northern localities but at Allendorph the insoluble content has increased.

Also, at Allendorph the algal content declines as does the micrite and microspar while the spar increases to its highest percentage in either unit of the Eiss Limestone. The previous characteristics of the Allendorph locality could indicate a shoal near the area. The shallower water would increase the bottom turbulence to the extent that the finer carbonate particles were winnowed away while insolubles were being poured into the area to the extent that they excluded algal growth either due to murky water or poor bottom conditions. The high percentage of sparry calcite at the Allendorph locality is due to the absence of micrite with remaining voids being filled with sparry calcite. The presence of a dismicrite texture and several noticeable pelecypod burrows at the Allendorph locality substantiate the shoal hypothesis. The shoal or its effects extended to the Strong City locality as indicated by a dismicrite texture and a high sparry calcite content. Algae had again become the dominant organism but all other characteristics at Strong City are the same as at Allendorph.

The algal shelly facies to the north in the upper Eiss unit is essentially the same as that of the lower Eiss unit with the exception of the shelly fauna. The upper unit appears to have less shelly fauna and more algae. The previous characteristics could indicate deeper water in the upper Eiss unit.

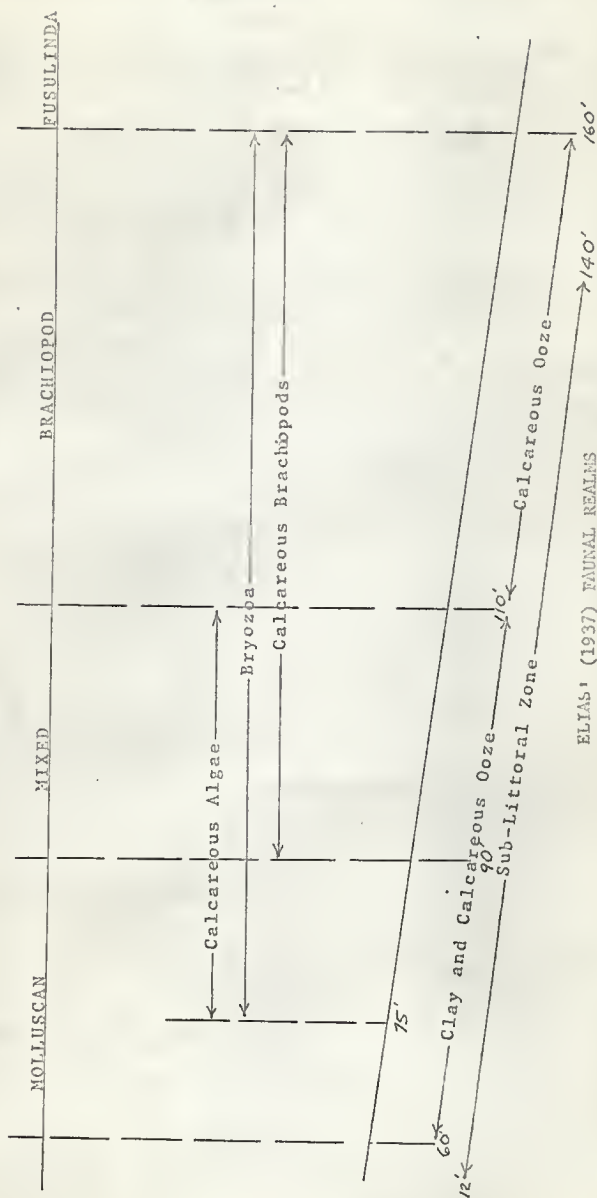
Petrographic Environmental Discussion

Elias (1937) in studying the Pennsylvanian-Permian sequences in Kansas noted their cyclothemic nature. In accordance with the lithology and faunal groups present Elias postulated several environments which could be used to differentiate carbonate sequences quite easily (Fig. 6). McCrone (1964) has demonstrated that Elias' original maximum depth of 160 feet can be compressed to 60 feet to explain most Kansas Wolfcampian cyclothemic facies. The writer agrees with McCrone in the choice of water depths and even believes that in some cases the water depth was less than three to five fathoms. The upper Eiss Limestone Allendorph locality would be a good example of the extremely shallow conditions mentioned above. Therefore, an alteration of Elias' original water depths produces an environment more suitable to the conditions of the Eiss Limestone (Fig. 7). It must also be kept in mind that even with slight water depth changes the shoreline of such a flat sea basin as that in Permian Kansas would have transgressed and regressed great distances, thereby controlling the terrigenous influx and contributing to vertical and lateral lithologic and biologic changes. The entire Eiss Limestone Member is an example of this fact.

EXPLANATION OF FIGURE 6

Elias' (1937) faunal realms for Kansas Pennsylvanian-Permian
cyclothem sedimentary.

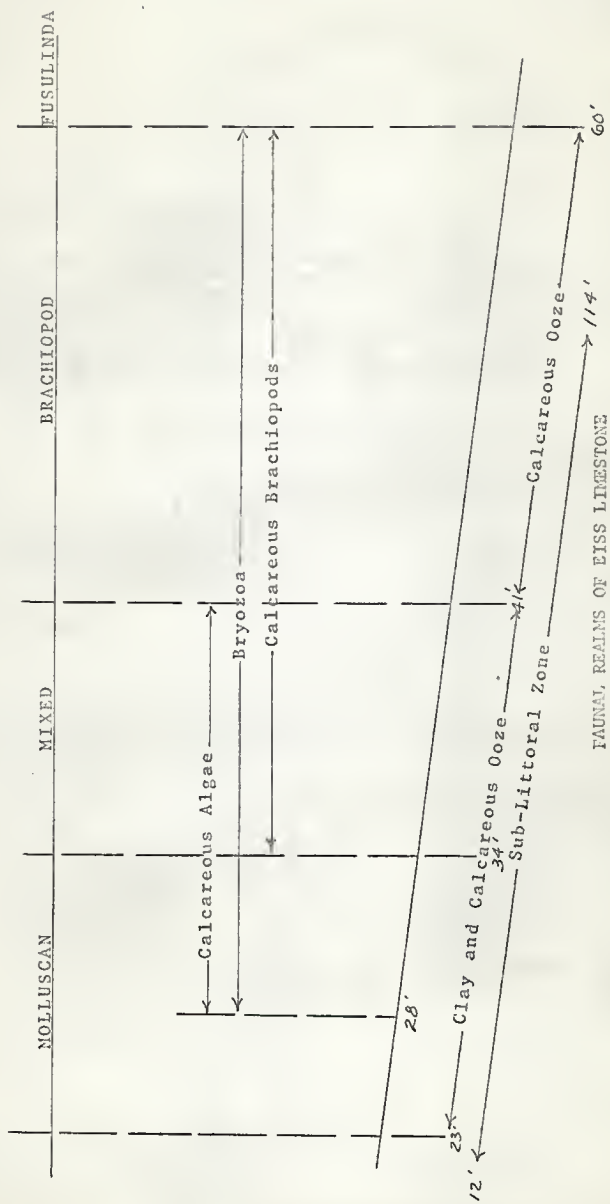
FIGURE 6



EXPLANATION OF FIGURE 7

McCrone's (1964) re-evaluation of Elias' (1937) original faunal realms. Elias' (1937) maximum depth of 160 feet has been compressed to 60 feet. The water depths and faunal assemblages in this environmental scheme are postulated for the Eiss Limestone.

FIGURE 7



CLAY MINEROLOGY

General Discussion

In order to obtain additional information concerning the source and depositional history of the Eiss Limestone, a rapid qualitative method of clay mineral identification was utilized. Using the standard method of X-ray diffraction techniques, each clay sample was scanned twice -- once untreated but oriented, and then treated with ethylene glycol for expansion studies.

The identification of basic clay minerals was made using the following characteristics (Grim, 1953, and Stindl, 1966):

ILLITE: basal spacing of 10 A.U. with submultiple basal spacings at 5 A.U., 3.3 A.U., and 2.0 A.U. The basal spacing at 10 A.U. was the strongest and subsequent glycolation did not affect the spacings.

CHLORITE: basal spacing between 14 and 15 A.U. with submultiple spacings at 7.15 A.U., 4.75 A.U., and 3.54 A.U. The first basal spacing at 14 A.U. was the strongest and subsequent glycolation did not affect the spacings.

MONTMORILLONITE: basal spacing of 12-14 A.U. is the strongest and upon glycolation will expand to 15-17 A.U. Several types of montmorillonite are undoubtedly present. The possible interlayered cation would be Ca or Na.

VERMICULITE: basal spacing of 14 A.U. is the strongest and upon glycolation will expand less than one A.U. The greater amount of expansion differentiated montmorillonite from vermiculite.

MIXED-LAYER: basal spacings in the range of 20-40 A.U. indicated mixed-layered clay minerals which are formed by the regular stacking of two or three different clay minerals. No attempt was made to differentiate the various mixed-layered clay minerals, therefore they will all be grouped together.

Geochemically the presence of substantial concentrations of several metal cations in the Eiss Limestone could be explained by their presence in the various clay minerals. Calcium is present in the montmorillonite structure but its low percentage would be masked by the high concentration of calcium in the carbonate minerals of the matrix. The presence of ferrous iron and magnesium as possible exchange cations could be expected, but the amount of these two elements in the final montmorillonite structure would be negligible. Calcium and magnesium may also replace interlayer potassium ions in the illite structure. It is possible that since the samples contain a high percentage of illite, a substantial percentage of magnesium in the oxide analyses could be explained here. The most significant exchange of cations is in the clay mineral chlorite. Magnesium and ferrous iron constitute a significant percentage in the chlorite structure, and manganese can successively replace either element. Geochemically

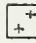


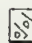
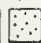
the presence and percentage of magnesium, ferrous iron, and manganese could be explained by the incorporation of chlorite into the Eiss Limestone clay fraction. Chlorite appears only in three samples but there is no correlation between its presence and any increased cation percentage. Magnesium and calcium are exchangeable cations in vermiculite, but vermiculite's random distribution does not correlate with the concentration of either cation. The mixed-layered clay minerals present can exchange any or all available cations since they consist of stacked, individual clay minerals.

Lower Eiss Limestone Unit

The lower Eiss Limestone unit is characterized by a suite of illite, montmorillonite and mixed-layered clays in the northern localities (Fig. 8). Further south at the Allendorph locality the montmorillonite and mixed-layered clays are absent while an illite, vermiculite suite is dominant. At the Strong City area the suite is mixed-layered and chlorite minerals. It is believed that two different sources are indicated; one north, the other south of the Allendorph area. The sources north and south of Allendorph are also noted in the petrography of the Eiss Limestone. Sedimentation from these two sources must have been greater in lower Eiss time than in upper Eiss time as evidenced by the consistently greater insoluble residue percentage in the lower Eiss Limestone.

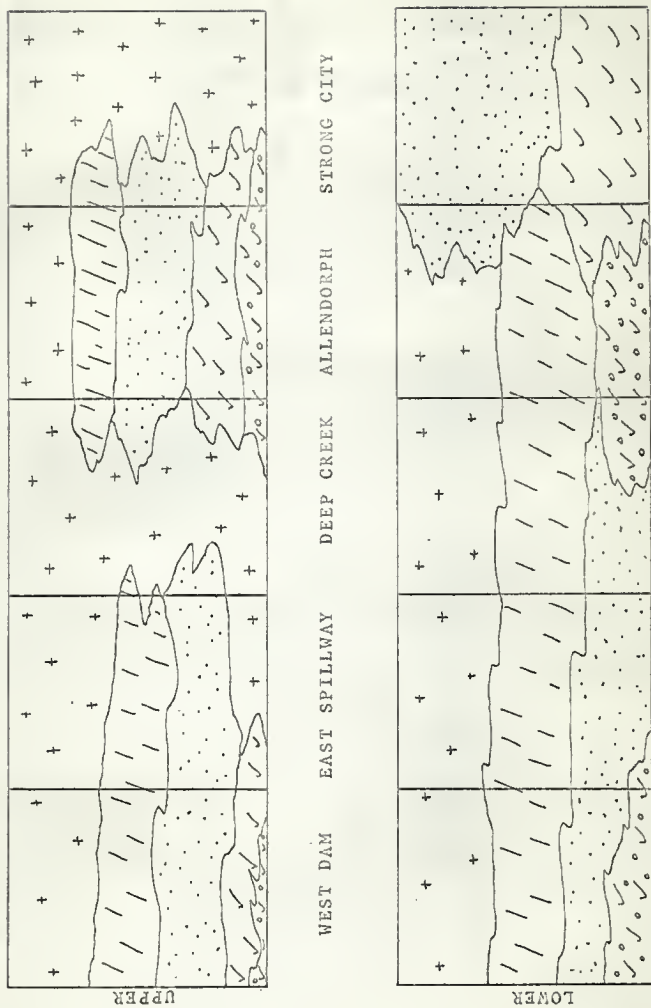
EXPLANATION OF FIGURE 8

Qualitative clay mineralogy of the Eiss Limestone.

	Illite
	Montmorillonite
	Chlorite
	Vermiculite
	Mixed-layered clays.

Clay minerals at each locality represent only the type present
not the percentage.

FIGURE 8



Upper Eiss Limestone Unit

The clay mineral suites of the upper Eiss Limestone are more ambiguous than those of the lower Eiss Limestone. The northern localities are essentially an illite, montmorillonite, mixed-layered suite which consistently decreases in clay mineral types until the Allendorph locality is reached. At the Allendorph locality five different clay minerals are present which could indicate the influence of two source areas mixing clays at that locality. The higher insoluble residue content at Allendorph further substantiates this hypothesis. Further south from Allendorph at the Strong City locality illite is the only clay mineral present which produces some ambiguity in relation to a southern source.

Stindl (1966) has shown that chlorite-montmorillonite and vermiculite-montmorillonite suites are characteristic of reworked sediments which are associated with the immediate source area. Both the upper and lower Eiss Dam and upper and lower Eiss Allendorph localities have a chlorite-montmorillonite and vermiculite-montmorillonite suite. The suggestion of a northern and a southern source is further substantiated by the previous suites of clay minerals.

CALCIUM AND MAGNESIUM GEOCHEMISTRY

Aragonite - Calcite Relationships

Calcium carbonate polymorphs, calcite and aragonite have been thoroughly examined by several authors (Graf, et al, 1955), and it appears that aragonite is thermally unstable with respect to calcite. Graf and Lamar (1955) have demonstrated that aragonite will remain stable for some time in a dry environment but the aragonite - calcite transition will proceed rapidly in hydrous environments and at elevated temperatures. Therefore, with time in most diagenetic environments aragonite will be eliminated. Murray (1954) stated that metal ions such as Pb, Sr, and Mg effect the particular polymorph that will be deposited. The presence of any of these metal ions enhances the formation of aragonite in preference to calcite and magnesium. The factors that control the precipitation of carbonate sediments and shells have been investigated by Zeller and Wray (1956). The latter found that temperature, pH, impurities in concentration, solubility, crystal size, and the time element all affect the polymorph problem. Of these it appears that the impurity ion concentration has the greatest control. But to consider one of these to the exclusion of the others seems erroneous. Water of a higher temperature enhances the precipitation of aragonite while water of a lower temperature produces calcite. Conditions of high pH in either shallow restricted marine basins or in shallow open marine water tend to produce carbonate rocks that contain

appreciable trace amounts of Sr, Ba, and Mg. It is also apparent that leaching affects Mg to a greater extent than either Sr, Ba, Fe or Mn, and that by only complete dissolution of the carbonate rock will the concentrations for the various latter elements be altered quantitatively.

Precipitation Mechanism

One of the most important and yet unproven questions in the realm of marine carbonate sediments, is that of the precipitative mechanism: by organic or inorganic means. In the earlier days of carbonate studies it was thought that direct chemical precipitation was the most logical explanation for the immense volume of carbonate sediments in the geologic column. Presently there appears to be a great question concerning the effect of organic chemical precipitation of carbonate rocks. Zen (1960) stated that the application of the open-sea deposition of carbonates to carbonate rocks in the sedimentary record show that many two-carbonate rock systems, which from geological evidence most have formed in open, shallow seas, cannot be the product of direct chemical precipitation.

In addition, Bass Becking, Kaplan, and Moore (1960) have demonstrated that reductive photosynthesis by algae and colored bacteria control the Eh-pH of the system and hence the carbonate precipitation. A photosynthetic mass, such as an algal mat, may raise the pH to 9.4 and, in the absence of bivalent cations, to 12.6. Therefore the Eh-pH characteristics are determined

chiefly by photosynthesis, respiration and by oxidoreductive changes in the system (particularly for Fe and S).

To exemplify the practicality of the previously postulated ideas concerning organic precipitation the author quotes Emery, Tracey, and Ladd (1954) on the geology of Bikini and nearby atolls.

"Living Lithothamnium form 90-100% of the marginal zone, but it covers only 5-10% of the whole reef surface and probably does not form more than 20% of the living, calcium - secreting organisms of the reef. Yet samples of rock from lagoon beaches may contain 30-50% of fine to coarse grains derived from Lithothamnium because of the rapid rate of growth of the algae, and because of its rapid comminution to coarse material by the reef and to fine material by the scraping of animals, and by the abundant boring animals that infest the living algae."

Also, Swinchatt (1965) stated that Halimeda produces a large volume of skeletal carbonates relative to the total weight of the algae. Therefore, one must not concern himself primarily with the direct chemical precipitation of carbonates without giving equal explanation to the effects of biochemical or organic precipitation.

The Role of Magnesium

In recent years quantitative studies have been made concerning the second most important constituent of limestone, magnesium, and its related minerals. In the skeleton of littoral organisms (Pilkey and Hower, 1960) a certain correlation has been suggested between shell composition and chemical and physical environmental factors, such as salinity and temperature. Goldsmith

(1959) reports that the high concentration of MgCO_3 in solid solution in many of the marine organisms is obviously a non-equilibrium state. For example a great number of calcareous algae contain a quantity of MgCO_3 in solid solution that would only be stable at temperatures upwards of 800°C .

In addition to temperature and salinity the phylogenetic level of the organism appears to be a contributory factor in the enrichment of an organism with respect to MgCO_3 . Some calcareous algae have been reported with about 30% MgCO_3 . Chave (1954a) states that the mineralogical form of the carbonate is the most critical in determining the amount of magnesium that can enter shell carbonates. In aragonites the magnesium level rarely exceeds 1% while biogenic calcites usually contain more than 1% and quite frequently as much as 20% to 30%. If MgCO_3 in marine organisms is in a state of non-equilibrium then the presence of Mg alone is even in a greater state of non-equilibrium. Chave (1954b) and Friedman (1964) showed that the most common change in the calcitic skeleton was the loss of Mg since high Mg calcite was more unstable than aragonite. But in the inversion of aragonite-calcite the Mg content remained unchanged and was found to be very low. Magnesium in fossils they found would reach equilibrium as:

- (1) Mg was removed from the fossil and deposited in the near-by matrix as dolomite or a similar Mg mineral.
- (2) Fossil material was reorganized to form two stable phases, low Mg calcite and dolomite.

(3) Magnesium was removed from the rock by circulating water. Of these three the first was believed to be the most significant and the second one the least. Chave (1952) also postulated additional evidence that the calcite-dolomite, i.e., Ca and Mg, solid solution was unstable. Analyses of fossil materials demonstrated that the Mg content fell to one or two per cent often within a few million years. The Mg is selectively replaced by calcium, and the forms richest in Mg seem to be changed first. The latter would suggest that the solid-solution series calcite-dolomite is unstable under all near surface conditions except within the biological environment which produced it.

The lack of an explanation concerning the "dolomite problem" lies in the failure of experimental dolomite precipitation at room temperature. While older geologists still believe in the syngenetic origin of dolomite the present consensus is that dolomites are a product of early diagenetic metasomatism of calcite. This idea can be proven through the use of stable matrix relationships (O^{18}/O^{16}) in mineral pairs such as calcite-dolomite (Degens and Epstein, 1964). Degens and Epstein have shown that in ancient marine dolomite-calcite pairs of penecontemporaneous diagenetic and epigenetic origin from the Precambrian up to the Tertiary:

- (1) All sedimentary dolomites, independent of age (at least for the last 1000 million years), environment, and mode of formation (whether syngenetic, diagenetic, or epigenetic) are products of $CaCO_3$ metasomatism.

- (2) Dolomitization always proceeds under solid state conditions without chemically altering the CO_3 -2 unit of the CaCO_3 precursor (it should be pointed out that for structural reasons aragonite first has to become inverted to calcite before dolomitization may proceed).
- (3) In contrast to calcite and aragonite, dolomite is very reluctant to adjust isotopically to changes in temperatures and to the $^{18}\text{O}/^{16}\text{O}$ ratio of formation water. This makes dolomite of marine origin a useful tool for the evaluation of paleo-temperatures in the ancient seas.
- (4) Late diagenetic-epigenetic dolomitization is frequently a two-step process. The original limestone first crystallizes into secondary calcite which subsequently is metasomatically replaced by dolomite. The occurrence of dolomitization patterns (i. e. veins) that cut across primary, sedimentary fractures can be explained this way.

It is not yet fully understood what type of environmental conditions have to exist for dolomites to be formed. Degens (1965) stated that the environmental formation of dolomites can be caused by one or a combination of the following:

- (1) high temperature ($> 200^\circ\text{C}$);
- (2) high chlorinity;
- (3) presence of aragonite or magnesium-calcite;
- (4) decrease of Ca/Mg ratio in the solutions.

From an evaluation of recent sediments in the Bahamas; Huron Reef, Australia; and Mexico, Friedman (1964) came to the conclusion that dolomite was formed in these environments in the recent situation by:

- (1) Penecontemporaneous sediment in the intertidal zone of pellet muds among algae mats.
- (2) Deep water marine conditions.
- (3) Replacement of calcite-infilled molds of originally aragonitic grains.

All of the above would be subject to metasomatism and the last example is probably a definition of in-plane metasomatism.

Recent evidence shows that clay minerals may effect the formation of some dolomite (Kahle, 1965). Clays may behave as catalysts providing a source of Mg ions or by serving as membranes which effect ionic migration. Alternatively, clay minerals may serve as the center of nucleation or by entering into chemical reaction which involve dolomite or one of the products. Magnesium in interlattice sites or in exchange positions is common in montmorillonite, chlorites and vermiculites which may contain 25 per cent or more magnesium oxide.

Calcium/Magnesium Ratios

In a geochemical attempt to utilize the two most abundant elements in sedimentary carbonate rocks, calcium and magnesium, several authors have shown that the ratio Ca/Mg can be used effectively. Chilingar (1956b) found no simple relationship

between the Ca/Mg ratio and the geologic age of carbonate rocks. He did, however, find a general decline in abundance of dolomites (or an increase in the Ca/Mg ratio) with decreasing age. Vinogradov, Ronov, and Ratynskiy (1957) found the same increase in Ca/Mg ratio with younger carbonate rocks characteristic of the Russian Platform carbonates. In working with recent carbonate environments Chilingar (1956b, 1960) found that the Ca/Mg ratio of the skeletal structures of invertebrates is proportional to the Ca/Mg ratio of the environmental medium. In other words the environmental sea water will control the Ca/Mg ratio to the greatest extent. Also, Chilingar demonstrated that in some recent localities the Ca/Mg ratio increases with increasing depth and distance from shore in the calcium sediments. Both the sediments of the Great Bahama Bank and the Persian Gulf have these characteristics. In some instances, the low Ca/Mg ratios near-shore can be attributed to the abundance of magnesium-bearing coralline algae in the near-shore water. Kahle (1965) suggested that the increase of magnesium from shore with increasing distance could be due to the magnesium content of clays which themselves increase away from shore. Hirst (1962) showed that the constancy of the Mg/Al ratio of sediments in the Gulf of Paria proved the presence of magnesium in the clay formation. Chilingar (1963) reported that the problem of determining an accurate Ca/Mg ratio in ancient carbonate rocks is the magnesium-clay relationship. He suggested that the clays be separated with little or no leaching in the laboratory and the matrix carbonate Ca/Mg ratio then

determined minus the clay. This is an excellent suggestion but what physical means available to the geochemist could separate the clay mineral fraction without leaching some magnesium from it?

It is most interesting to note the relationship between the insoluble content of carbonates and the principal ions. Bisque and Lemish (1959) demonstrated the significant relationships that the greater the amount of insoluble the greater the amount of magnesium as $MgCO_3$ and the greater the FeO the greater the magnesium. The latter was performed on the Devonian Cedar Valley Formation. In a later paper concerning the same subject but in the Lockport Formation (Niagaran) of New York State, Zenger (1965) demonstrated that there was no relationship whatever between the calcite-dolomite ratios and the insoluble residue. It is significant that the article by Zenger used X-ray diffraction peaks of calcite-dolomite while Bisque and Lemish wet chemically determined the magnesium present and directly placed all of it in the dolomite structure. Several interesting points are to be noted here. If one concludes that all magnesium in the carbonate is in the form of dolomite then the existence of a high - Mg calcite or Mg-clay minerals must be ruled out. Also, the method of obtaining quantitative X-ray diffraction percentages of calcite and dolomite constitutes an error of at least 10% with a minimum detectability of at least 4%. Therefore, it would appear that both methods have areas of inaccuracy and the methods and postulations need to be more quantitatively approached. Others involved in the insoluble-dolomite question such as Fairbridge (1957) propose that

the characteristically high insoluble dolomites were deposited closer to shore than the undolomitized limestone. Chilingar's postulation of the Ca/Mg ratio increasing with increasing depth and distance from shore supports this assumption. High insolubles could be due to drainage systems entering the sea rather than the distance off shore. Also, selective leaching of calcite would decrease the Ca/Mg ratio and at the same time increase the insoluble residues. Steidtmann (1917) suggested that although mixed carbonates (dolomitic limestones and calcium dolomites) were in the minority, they tended to have a higher acid-insoluble content than true limestone or dolomite samples. In other words the Ca/Mg, dolomite and insoluble residue relationships are still in a confused state.

Eiss Limestone Ca/Mg Consideration

Mineralogically both the upper and lower Eiss Limestones are monomineralic (calcitic) with the exception of five samples. The increase in Mg content in these five samples is directly proportional to the dolomite content as determined by X-ray diffraction.

	<u>Sample No.</u>	<u>ZMg++</u>
	1087b (L)	0.556
	1086b (L)	0.784
	1087a (L)	1.926
	1084 (U)	2.876

↑
decrease in X-ray
dolomite content

Therefore, the writer believes that the magnesium in the Eiss Limestone is in the form of dolomite and not magnesium clay minerals. The dolomite was found texturally to be dolomicrite to dolomicrospar.

On the basis of insoluble residue percentages and Ca/Mg ratios (Fig. 9) it is possible to differentiate geochemically the upper and lower Eiss Limestones. The lower Eiss Limestone has a definitely higher insoluble residue percentage and a slightly lower Ca/Mg ratio than the upper Eiss Limestone. This could possibly indicate that the upper Eiss Limestone was deposited in deeper water and further from shore than the lower Eiss Limestone. It is therefore suggested that the Ca/Mg relationships of the Eiss Limestone can be used with reservation in separating the upper from the lower limestone. There appears to be no definite trend in the strike direction of either limestone in relation to Ca/Mg ratios although the lower limestone perhaps suggests lower values to the north. This could indicate shallower water to the north but a definite trend is not indicated. Therefore, both limestones probably were of different depths and possibly distances from shore with occasional fluctuation along the strike direction.

Ferrous iron percentages versus magnesium percentages (Fig. 10) indicate a striking separation of upper Eiss from lower Eiss Limestone. While the magnesium values for both fall in the range of 0.3 to 0.8 per cent (excluding two high dolomite samples), the ferrous iron content separates the upper Eiss from the lower Eiss at approximately 0.22 per cent ferrous iron. Hence any value below 0.22 per cent would be most likely characteristic of the upper Eiss unit while higher values would indicate lower Eiss

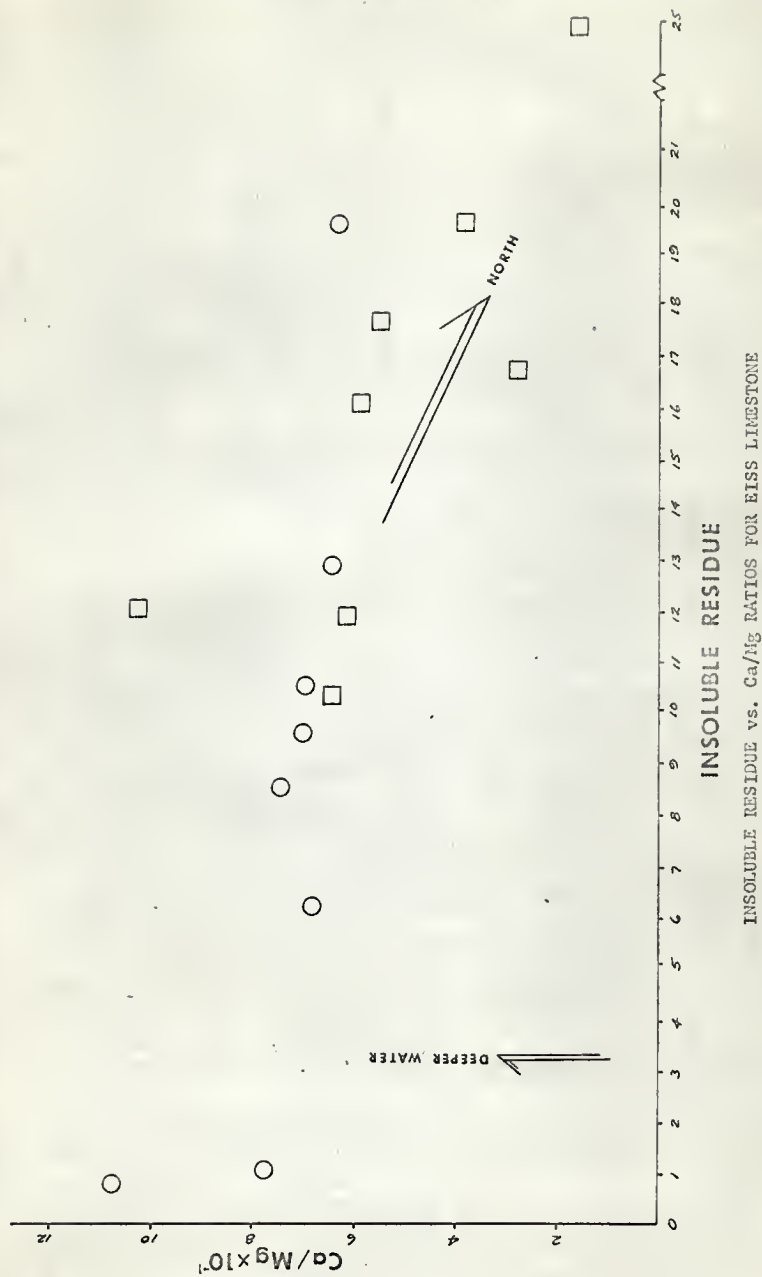
EXPLANATION OF FIGURE 9

Per cent insoluble residue plotted against Ca/Mg ratios for the
Eiss Limestone.

☐ Lower Eiss Limestone

☐ Upper Eiss Limestone

FIGURE 9



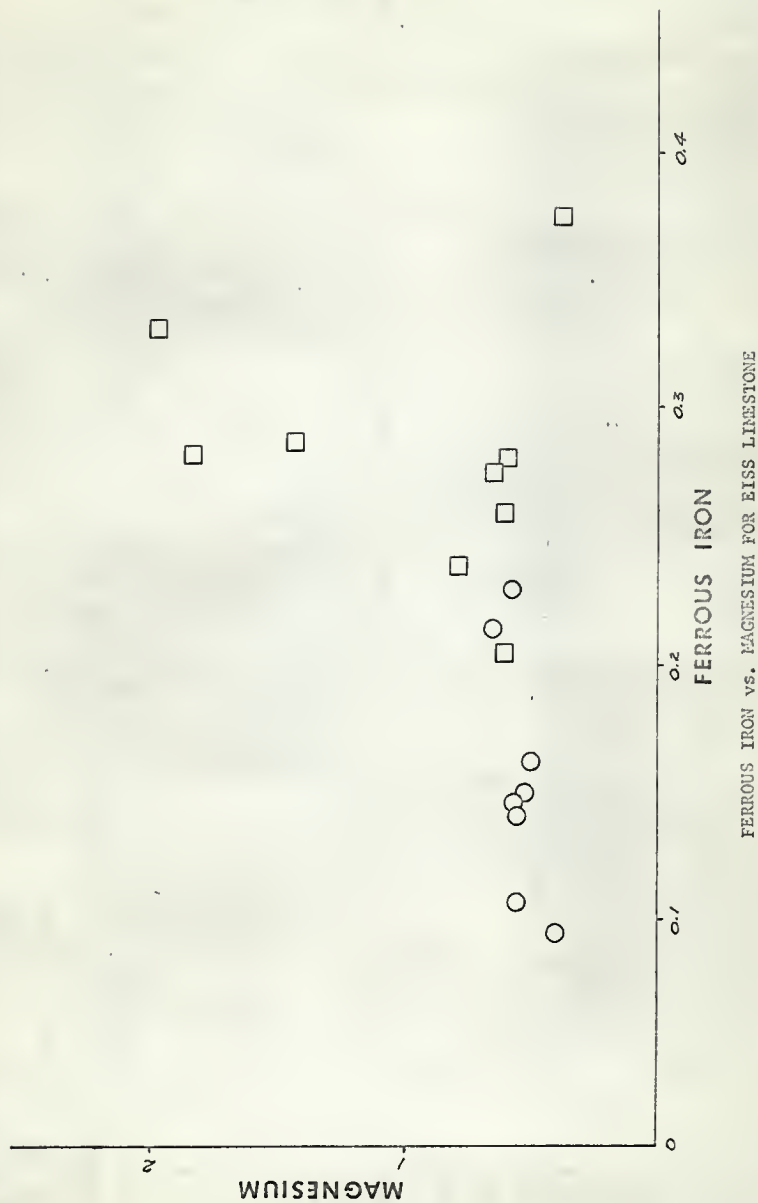
EXPLANATION OF FIGURE 10

Per cent ferrous iron plotted against per cent magnesium for the Eiss Limestone. High magnesium samples contain dolomicrite and dolomicrospar.

□ Lower Eiss Limestone

○ Upper Eiss Limestone

FIGURE 10



Limestone. This relationship could be explained in the light of insolubles which contain more iron-rich clays in the lower Eiss than in the upper Eiss as demonstrated by X-ray diffraction studies.

STRONTIUM GEOCHEMISTRY

Most of the Sr in limestone occurs in Ca sites in the calcite and/or aragonite structure. In environments of evaporate conditions smaller amounts of Sr precipitate as SrCO_3 , strontionite. The sulfate form of Sr is also present in some carbonates in the form of celestite, SrSO_4 ; but, like barite, it generally is formed by secondary processes. In evaluating true depositional Sr, celestite contamination poses a problem of a false increase in local concentration.

Turekian and Kulp (1956) demonstrated that the Sr content of carbonate fossils and sediments was a function of the following:

- (1) Sr/Ca ratio of the liquid environmental phase.
- (2) The particular polymorph, calcite or aragonite, which houses the Sr.
- (3) The vital effect of the organism.
- (4) Temperature.
- (5) The salinity of the liquid environmental phase.

Lowenstam (1953) concluded that the Sr/Ca ratio in organisms with mixed aragonite and calcite tests is a function of the percentages of these two polymorphs present. The amount of aragonite present is temperature dependent, and in a high temperature (i.e. tropical) area a greater amount of aragonite than calcite will be formed. It is also apparent that the aragonite structure accepts the Sr atom more readily than that of the calcite. Therefore, the greatest amount of Sr should occur in warm water environments.

Both Lowenstam (1953) and Turekian (1955) concluded that the salinity as well as temperature is an important factor in determining the Sr/Ca ratio.

The value and significance of the Sr/Ca atomic ratio demands careful consideration. The Sr/Ca atomic ratio as defined by Odum (1950) is (Sr/Ca) 1000. By a thorough investigation of the Sr/Ca ratio in carbonate rocks and fossils several authors have indicated trends in the geochemical ratio of these two elements. Table 8 presents a scan of the Sr/Ca ratios. From the data several possible correlations are suggested:

- (1) The average value of (Sr/Ca) 1000 for all samples studied is 0.71.
- (2) Fossils contain in the average twice as much Sr as the surrounding matrix.
- (3) Fossil ratios vary depending on the salinity and composition of aragonite to calcite in the original shell.
- (4) Both matrix and fossil ratios will be lessened if recrystallization has occurred.
- (5) Similar marine environment is evidenced by the constancy of Sr content of a long range genus of fossils.
- (6) Temperature of the ocean water is a relatively unimportant feature for the determination of the Sr content of fossils.
- (7) There is no evidence for seasonal fluctuations in Sr content.

Table 8

Variations in Strontium and Sr/Ca Ratio

Location Age & Occurrence	(Sr/Ca)1000	Comments	References
Cam. ls. matrix	0.25	Wyoming	Kulp <u>et al</u> (1952)
Ord. ls. matrix	0.95	Texas	Ibid.
Sil. ls. matrix	1.19	New York	Ibid.
Triassic ls. matrix	2.00	Calif., Nev.	Ibid.
Average of fossil species	1.03	Varying ages	Ibid.
Average of matrices	0.51	Varying ages	Ibid.
Average of 155 ls.	0.71	Varying ages	Ibid.
Average of 40 ls.	1.21	Varying ages	Odum (1950)
Range 78 Paleozoic ls.	0.11-3.90	Varying ages	Kulp <u>et al</u> (1952)
Average 78 Paleozoic ls.	0.76	Varying ages	Ibid.
Range 25 Paleozoic ls.	0.3-1.4	Varying ages	Odum (1950)
Average 25 Paleozoic ls.	0.9	Varying ages	Ibid.
Average of 155 fossils from Calvert Fm	3.10	Miocene	Kulp <u>et al</u> (1952)
Average 103 unre- crystallized fossils	2.76	Varying ages	Ibid.
Average 198 all fos- sils studied (includes many recrystallized)	1.88	Varying ages	Ibid.

Table 8 (continued)

Location Age & Occurrence	(Sr/Ca)1000	Comments	References
<u>Cases</u>			
<u>Venus</u>	3.0	Miocene	Kulp <u>et al</u> (1952)
<u>Venus</u>	3.1	Miocene	Odum (1950)
<u>Pectin</u>	2.1	Miocene	Kulp <u>et al</u> (1952)
<u>Pectin</u>	2.5	Miocene	Odum (1950)
<u>Dentalium</u>	3.8	Miocene	Kulp <u>et al</u> (1952)
<u>Dentalium</u>	2.4	Miocene	Odum (1950)
Recent invertebrate sand	10.89-13.00	Bikini coral & <u>Halimeda</u> sand	Odum (1950)
Deep sea sediments	1.49-1.94	Indian and Pacific Oceans	Thompson & Chow (1956)
Strontinite deposits	6.750	Washington State	Ibid.
Present ratio of sea H ₂ O	8.90	Varied samples	Siegel, F. R. (1961)

- (8) A decrease of the Sr/Ca ratio with time from the Permian to the Tertiary (this was not found in North American carbonate rocks, only Russian Platform carbonates).
- (9) Within a narrow stratigraphic range the Sr content does not vary from the average.

A great deal of speculation concerning the correlation of Sr/Ca ratios in relation to the geologic column in the literature is present. Vinogradov et al (1952) found a general increase in the Sr/Ca atomic ratio from the Permian to the Tertiary for carbonate rocks of the Russian Platform. Murray (1954) also noted the general increase in Sr/Ca atomic ratio with geologic time and concluded that the phenomena was due to Sr substitution in aragonite relative to calcite. For instance, in the Paleozoic the Sr/Ca atomic ratio of the sea water was low and permitted the formation of calcite relative to aragonite. The invertebrate organisms at this time therefore deposited CaCO_3 in their tests in the form of calcite. At the end of the Paleozoic the Sr/Ca atomic ratio had increased in sea water and organisms with aragonitic tests had become more pronounced. The aragonitic precipitation of invertebrate organisms still persists today. Hence, the increase in the Sr balance of sea water from Precambrian times to recent may have been a factor in the evolution of marine invertebrates. Turekian and Kulp (1956) agree generally with the ideas of Murray but believe that the basic change of increase in the Sr content of sea water was due to the changes in the types of rocks exposed to weathering.

They suggest that the Paleozoic sediments received Sr from the basaltic rocks from the continent while during the Mesozoic to Recent periods, granites and granodiorites were the source. A correlation of Sr/Ca atomic ratios with type source rocks is shown by the following data:

Rock Type	%Ca	ppm Sr	Sr/Ca 1000
Basaltic rocks (245)	7.1	465	6.5
Granitic rocks (175)			
0.1 - 1.0% Ca	0.6	100	16.7
1.0 - 5.0% Ca	1.9	440	23.0

Turekian and Kulp (1956)

Until further research is performed on the problem of Sr/Ca atomic ratio fluctuations with time one can only accept the trend without knowing why.

While the Sr/Ca atomic ratio does increase with time several attempts have been made to present an average value for the Sr content of various carbonate rocks and sediments. For the sake of a relative Sr value and a workable average the data is outlined in Table 9. A workable Sr range from the previous data would be from 460 ppm Sr to 610 ppm Sr for most limestones. Since errors are involved, a ± 50 ppm variance should be attached to the maximum and minimum of the Sr range.

One of the problems of Sr analyses in limestones is the effect of recrystallization on the Sr balance. Goldberg (1957) stated that fossil Sr/Ca atomic ratios would be lowered upon

Table 9

Average Strontium Content for Carbonate Matrices

Matrix	Sr Content	Comments	References
Limestone	600 ppm	Penn. fresh & marine	Keith & Degens (1959)
Sed. $\text{CO}_3^{\text{--}}$ x	475 \pm 50 ppm	Various $\text{CO}_3^{\text{--}}$'s	Ingerson (1962)
Limestone	440 ppm	Misc.	Graf. (1960)
Limestone	610 ppm	150 various samples	Turekian & Kulp (1956)
	617 ppm	Computer derived (theoretical)	Horn & Adams (1966)

recrystallization. This will be apparent if the original Sr/Ca values are lower than those of sea water and then recrystallization takes place in nonmarine water. But on the other hand, if recrystallization takes place in a marine aqueous environment, then the subsequent Sr/Ca values could be increased instead of decreased. Vinogradov et al (1952) attributes the increase of the Sr/Ca values for Russian Platform carbonates to the fact that the Sr loss during recrystallization in general was not retained locally in the form of celestite. Sternberg et al (1959) attributes the variance in the Sr values of the Steinplatte reef complex of Austria to a loss of Sr during recrystallization. Therefore, it is apparent that during the recrystallization of a limestone the Sr content will be lowered and only with good petrographic control can one evaluate the characteristic Sr balance. In carbonates that have been subject to recrystallization, it is almost impossible to determine the original Sr content; and the Sr content can only be inferred from existing data for unrecrystallized limestones.

In an effort to relate Sr/Ca atomic ratios and Mg contents of Recent carbonate sediments Siegel (1961) proposed a relationship between the Sr/Ca ratio - Mg values and the distance from either a Pleistocene reef or a living reef. It was noted that the Sr/Ca ratio of the sediments increased away from the Pleistocene reef as the living reef is approached. At the main line of the living reef the Sr/Ca values decreased as they did in the open water seaward. Magnesium appeared to decrease as the Sr increased and reach a minimum when the Sr values reached a maximum. In relation

to fossil suites the sediment was composed of calcitic remains such as foraminifera, echinoids, and molluscs where the Sr was low and the Mg high. Conversely, for sediments of high Sr and low Mg, aragonitic reef material such as coralline fragments, algae and mollusc shells, predominated. Molluscan debris can appear in both types of sediment since the shells are composed of calcite, aragonite or mixed types. Where the Sr and Mg values appeared to be equivalent, the above mentioned fossil suites were averaged. Siegel's suggestions are quite interesting to the geochemist and could be of great value as are the Ca/Mg ratios and their relationship to depth of water and distance from shore. Further work is a necessity in relation to ancient carbonate rocks and will be valid only if the recrystallization - Sr loss problem can be solved.

Eiss Limestone Sr/Ca Consideration

The Sr content of the Eiss Limestone is contained in the matrix carbonates and not in associated Sr minerals. The absence of strontionite and celestite in the Eiss Limestone supports this conclusion.

The values of Sr obtained from the Eiss Limestone indicate a definite loss of Sr due to recrystallization. Petrographically both the upper and lower Eiss Limestone have been recrystallized with the exception of the upper Eiss Limestone at the Strong City location. Geochemically the Strong City upper Eiss Limestone (Fig. 11) is definitely different from the other Eiss locations.

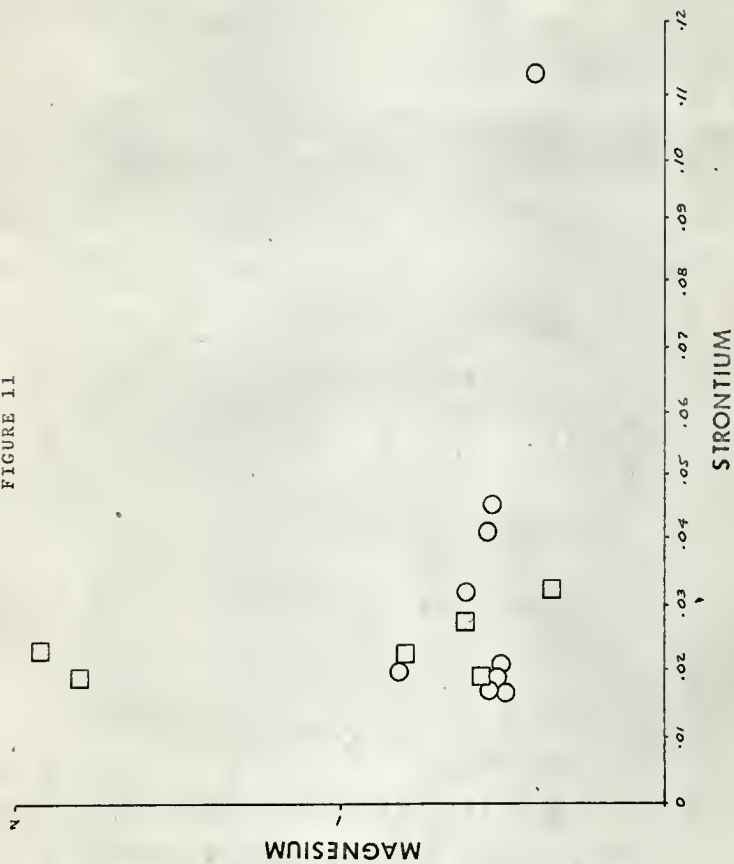
EXPLANATION OF FIGURE 11

Per cent magnesium plotted against per cent strontium for the Eiss Limestone. High magnesium values represent dolomicrite and dolomicrospar.

□ Lower Eiss Limestone

○ Upper Eiss Limestone

FIGURE 11



MAGNESIUM vs. STRONTIUM FOR THE EISS LIMESTONE

The average Sr content of the recrystallized limestones in the Eiss at all other locations is in the range of 160 to 450 ppm with an average of 220 ppm. The upper Eiss Sr value at Strong City is 1120 ppm which may indicate the possible true Sr content of the Eiss Limestone. Although the upper and lower Eiss Limestone cannot be separated on the basis of Sr versus Mg contents, the Sr values can be used as an index of recrystallization.

A very careful examination of the average Sr values for the upper and lower Eiss Limestone plotted against location (Fig. 12) yield some interesting results. Both the upper and lower limestones in the northern area have low Sr values with an average Sr ppm content that for all purposes is the same. As the limestones are traced south however, the Sr contents vary greatly and also increase rapidly. One can postulate that the effect of recrystallization was less extreme in the southern outcrop areas while both upper and lower limestones were highly recrystallized in the northern area. This postulation is borne out by petrographic evidence which tends to indicate more complete recrystallization in the northern area. But if one considers the Sr variations to be indicative of original environmental conditions several possibilities are available which are supported by data other than the Sr values. An increase in the Sr values toward the southern area could indicate two mechanisms of additional Sr. First a source of high Sr waters (i. e., high Sr pre-Eiss sediments) could have occurred to the south. The leaching of these sediments would have increased the Eiss waters in Sr content nearest the Sr source.

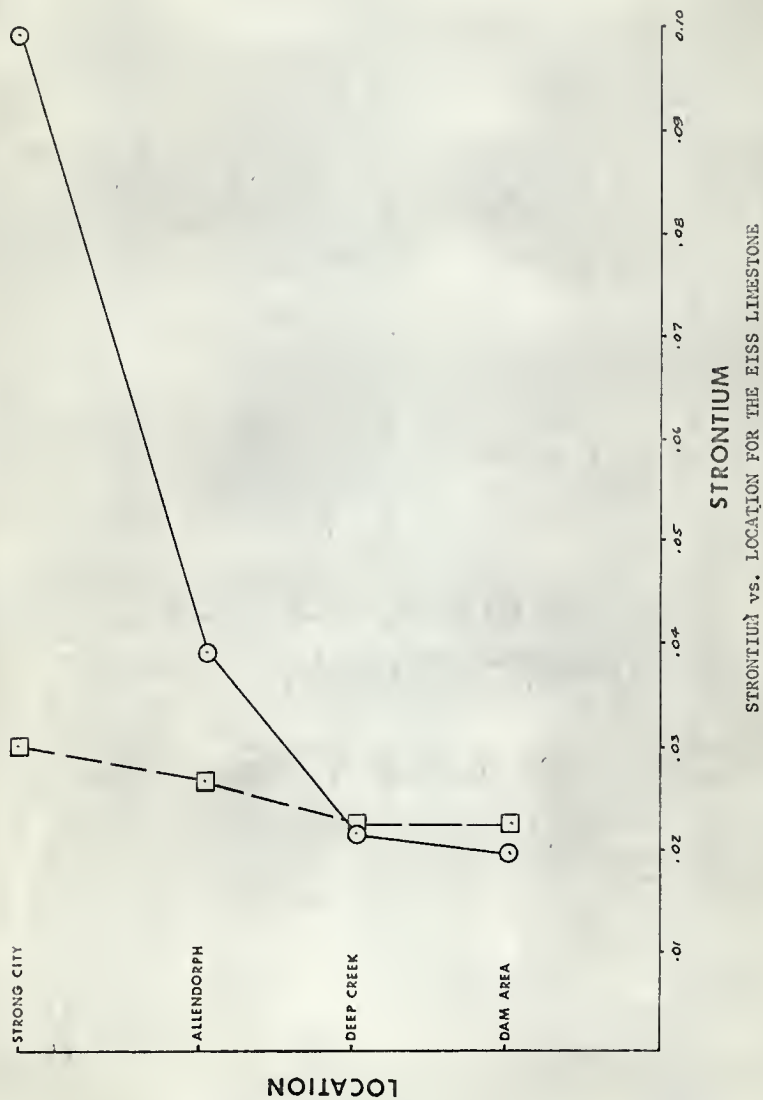
EXPLANATION OF FIGURE 12

Strontium ppm values plotted against sample locality for the Eiss Limestone. Note increase in strontium content to the south and relative equality of the strontium values to the north.

□ Lower Eiss Limestone

○ Upper Eiss Limestone

FIGURE 12



Secondly, a living reef could have occurred to the south which would add Sr to the water due to a high percentage of aragonitic organisms within it.

Until the value of the Sr analyses in relation to the mechanism of recrystallization is fully understood the carbonate geochemist cannot use Sr as a criterion of environment with any certainty. The use of Sr as an environmental indicator in this thesis can be effective only if coupled with the other data and only then can it be used with reservation.

Strontium Isotopic Analyses

Four isotopes of strontium exist: Sr^{84} , Sr^{86} , Sr^{87} , and Sr^{88} . Of these, Sr^{87} is produced by radioactive decay of Rb^{87} (with a half-life of 4.7 to 5.1×10^9 years). Therefore, since the age of the earth is 4.55 billion years old, it is possible to use Sr^{87} as a means of determining the age of rocks and minerals since we have both Rb^{87} and Sr^{87} in geologic systems. Since sedimentary carbonate rocks contain very little Rb, a relative rather than an absolute time measurement can be determined by measuring slight increases in Sr^{87} with time. By knowing the stratigraphic relative ages (i. e., Lower Permian, Middle Ordovician) one can determine the $\text{Sr}^{87}/\text{Sr}^{86}$ ratio or initial ratio and use this as being characteristic of that age material. This is possible since Sr^{87} relative to Sr^{86} increases as an almost linear function of time at a rate proportional to the decay of Rb^{87} .

If we consider the primordial value of $\text{Sr}^{87}/\text{Sr}^{86}$ of the earth to be equal to the value of meteorites (i.e. $\text{Sr}^{87}/\text{Sr}^{86} = 0.698$), our lower relative age and low initial ratio limit of the marine $\text{Sr}^{87}/\text{Sr}^{86}$ geochron is defined (Fig. 13). For an upper limit the value of modern day sea water is used which gives a $\text{Sr}^{87}/\text{Sr}^{86}$ ratio of 0.7093 (Faure, Hueley, and Powell, 1965). If our assumptions are correct the values of $\text{Sr}^{87}/\text{Sr}^{86}$ for all sedimentary carbonate rocks should fall between these maximum and minimum points. As indicated by the marine geochron, the values do fall between these two points.

Twenty carbonate initial ratio analyses of Kansas Permian limestones have been made at Kansas State University. These results along with previous determinations by several authors are presented in Table 10 and their relation to the $\text{Sr}^{87}/\text{Sr}^{86}$ marine geochron is seen in Fig. 13.

EXPLANATION OF FIGURE 13

Marine $\text{Sr}^{87}/\text{Sr}^{86}$ geochron including values for the Eiss
Limestone. Primordial $\text{Sr}^{87}/\text{Sr}^{86}$ in meteorites 0.6980; present day
sea water value 0.7093.

FIGURE 13

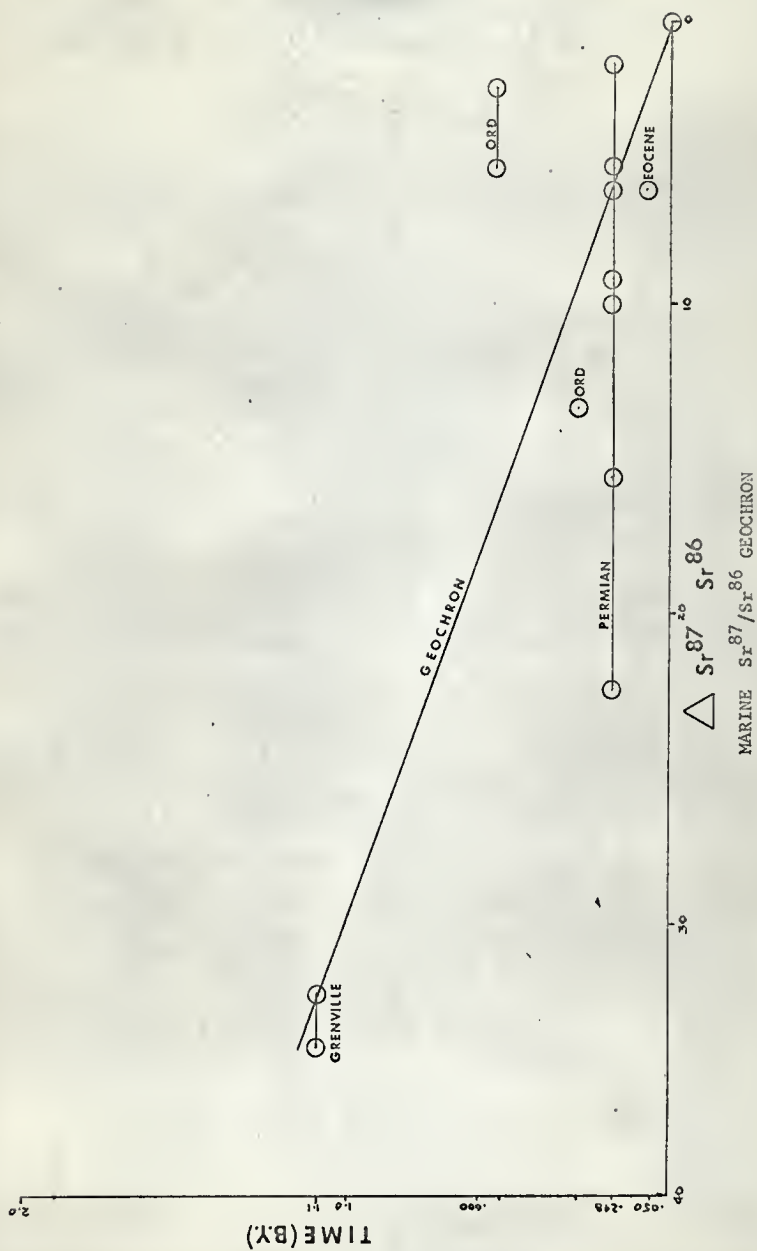


Table 10

Strontium Initial Ratio Analyses Summary

Formation	Age	Sr^{87}/Sr^{86}	$\Delta Sr^{87}/Sr^{86}$	Reference
Cresswell Ls.	Perm.	0.7075	-15.0	Brookins (1966)
Towanda Ls.	Perm.	0.7087	- 6.0	Ibid.
Threemile Ls.	Perm.	0.7086	- 7.0	Ibid.
Threemile Ls.	Perm.	0.7083	-10.0	Ibid.
Eiss Ls.	Perm.	0.7076	-17.0	Dowling (1967)
Eiss Ls.	Perm.	0.7084	- 9.0	Ibid.
Eiss Ls.	Perm.	0.7091	- 2.0	Ibid.
Eiss Ls.	Perm.	0.7078	-15.0	Ibid.
Eiss Ls.	Perm.	0.7083	-10.0	Ibid.
Eiss Ls.	Perm.	0.7070	-23.0	Ibid.
Newland Ls.	Beltian	0.7070	-23.0	Gast (1960)
Limestone (Haiti)	Eocene	0.7086	- 7.0	Hedge and Walthall (1963)
Limestone (Texas)	L. Ord.	0.7087	- 6.0	Ibid.
Limestone (Quebec)	Trenton	0.7090	- 3.0	Powell <u>et al</u> (1965a)
Limestone (USSR)	Ord.	0.7097	+ 4.0	Herzog <u>et al</u> (1958)
Limestone (Texas)	Ord.	0.711	+ 7.0	Gast (1960)
Limestone (Mich.)	Pref.	0.7058	+35.0	Personal communication Dr. Sam Chaudhuri (1967)

IRON AND MANGANESE GEOCHEMISTRY

General Discussion

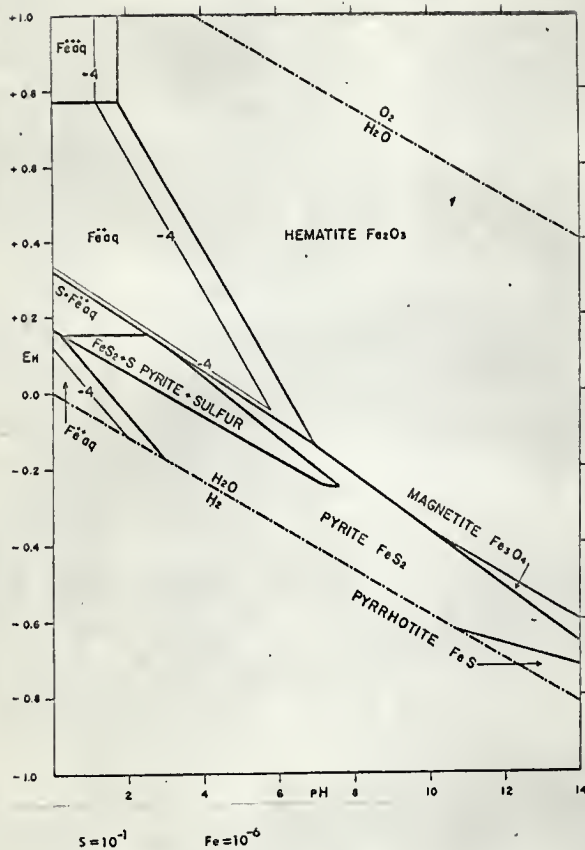
The close geochemical similarity of ferrous iron and manganese requires that these two elements be discussed together. In addition, the ferric iron-manganese relationship is also quite similar. The similarity is reflected geologically in their common occurrence in rocks of every type. The removal of iron and manganese from these rocks takes place during the various weathering processes. For most crystalline rocks the Mn/Fe ratio falls between 1/25 to 1/50. The ionic radii of Mn^{2+} and Fe^{2+} are almost identical; and therefore, they can substitute freely for each other in various structures. For the latter reason it is not expected that manganese will be leached preferentially with respect to iron, leaving the iron behind, since similar solution kinetics are to be expected for both elements.

A fractionation of these two elements is expected in nature since we find sedimentary manganese deposits, sedimentary iron deposits and sediments with extremely high or low Mn/Fe ratios. The most possible mechanisms for the fractionation processes are environmental pH and Eh fluctuations. Garrels and Christ (1965) have presented the stability diagrams for the manganese and iron carbonates, oxides and hydroxides (Figs. 14 and 15). Krauskopf (1957) concluded that at any given pH iron oxides and hydroxides precipitate at a lower Eh than do manganese oxides. Conversely,

EXPLANATION OF FIGURE 14

Eh-pH iron stability diagram.

FIGURE 14

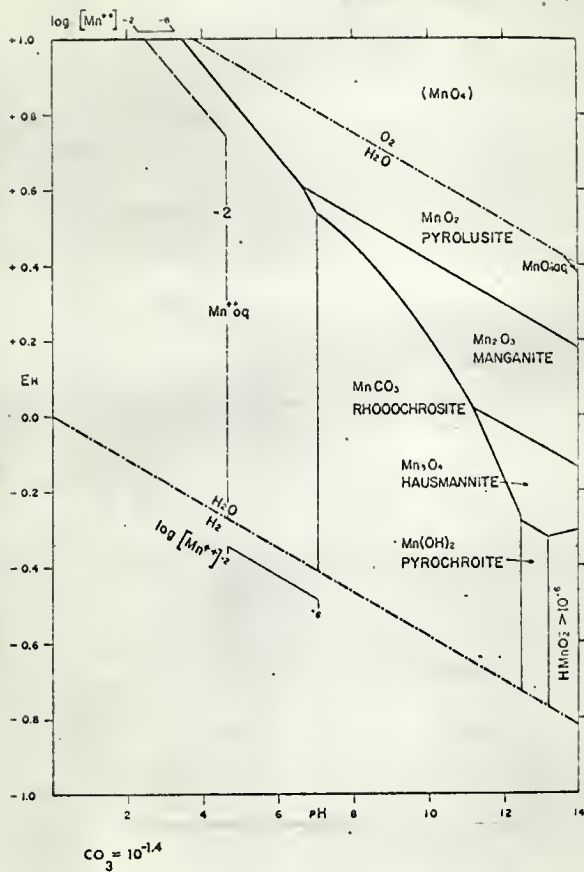


IRON STABILITY DIAGRAM

EXPLANATION OF FIGURE 15

Eh-pH manganese stability diagram.

FIGURE 15



MANGANESE STABILITY DIAGRAM

at any given Eh, iron begins precipitation as an oxide at a lower pH than does manganese. If carbonates can be precipitated then both elements will be precipitated at the same time due to the near equality in their solubility product constants for $\text{RCO}_3 = \text{R}^{++} + \text{CO}_3^{--}$. Thus a separation of the two elements is expected in almost every environment except when they are deposited as carbonates in the region of the carbonate stability field.

Mineral assemblages in the iron mineral stability diagram (Fig. 14) are very important and can indicate environmental conditions. Generally, hematite is the stable phase under oxidizing conditions while magnetite and siderite form under intermediate to moderate reducing conditions. In alkaline conditions magnetite will form before siderite. Pyrite requires moderate to strong reducing conditions while pyrrhotite requires even stronger reducing conditions.

Mineral assemblages in the manganese mineral stability diagram (Fig. 15) are also indicative of environmental conditions. The pH of the manganese system is more critical than the Eh in determining the final product. If the pH is below 7.0 then Mn ion will be the dominant species; but above a pH of 7.0 the carbonate, rhodochrosite, is dominant in both oxidizing and slightly to moderate reducing conditions. Only in fields of high pH and high Eh do the other manganese minerals play an important role.

The relationship of iron to the clay mineralogy of a carbonate has been previously discussed. It is also of importance that as

the substitution of Mn for Fe is possible in sedimentary environments that the clays could contain a substantial percentage of Mn in the substituted position of iron.

Hewett (1933) stated that although manganese was present in all animals and plants that only bacteria and algae tended to concentrate manganese since they precipitated it from solution. Therefore, it is quite possible that organic fractionation of iron and manganese could play an equally important role in sedimentary environments containing both of these elements. Hewett also concluded that pure non-magnesium limestones rarely contain more than 0.1% MnO while magnesian limestones contain more manganese with the amount increasing as the content of ferrous carbonate increases. Carbonate rocks which contain less than 1 per cent ferrous oxide commonly contain 0.1 per cent manganese oxide, but where ferrous oxide exceeds 20 per cent, manganese oxide is rarely less than 0.7%.

Graf (1960) stated that the average Mn content of over ten thousand specimens of Russian Platform carbonates yielded 530 ppm. This value can be compared with 490 ppm for sands and silts and 580 ppm for clays. The differentiation of carbonate rocks formed in humid and arid climates was proposed by Ronov and Ermishkina (1959) who stated that for humid climates the average Mn content was 810 ppm, while for arid climates the average Mn content was 320 ppm. They also correlated these values quite well with the amounts of Fe and insoluble residue. Graf (1960), in using the ratio $\frac{\text{MnO}}{\text{FeO} + \text{Fe}_2\text{O}_3}$, demonstrated what he termed "a geochemical

separation of Mn and Fe in zones of carbonate sediment accumulation." The average value of the ratio for carbonate rocks was 0.040 while for clays, sands, silts, and various igneous rock types it was between 0.011 and 0.024. Only through a complete program of manganese and iron investigation can the geochemist accept the data he is confronted with at the present time. Suggestions can be made but empirical statements should be avoided.

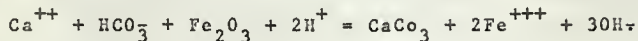
Eiss Limestone Fe/Mn Considerations

In the Eiss Limestones ferric iron is a post-depositional secondary product of ferrous iron oxidation with some primary pre-depositional ferric iron possibly still in the system. Pellets in the northern sections are characteristically coated with an iron stain. It is postulated that this stain is primary Fe_2O_3 which was formed in the aqueous environment of carbonate deposition. One might suggest that the Fe_2O_3 was derived from free ferric ions or from primary ferrous iron. The production of Fe_2O_3 in an aqueous environment with Ca^{++} , HCO_3^- and free Fe^{++} is strong:

$$\text{Ca}^{++} + \text{HCO}_3^- + 2\text{Fe}^{++} + 3\text{H}_2\text{O} = \text{CaCO}_3 + \text{Fe}_2\text{O}_3 + 7\text{H}^+ \quad G_r' = (-) 114.9 \text{ kcal/m.}$$

Therefore, the formation of Fe_2O_3 around the pellets could be due to the oxidation of ferrous iron, but why only in this position? Why does not the Fe_2O_3 occur in the pellet or in the matrix which is nearest to it? The author believes that this could be due to primary accumulation of Fe_2O_3 in a predepositional environment. It had to have been pre-depositional since Fe^{+++}

could not have been derived from existing Fe_2O_3 in either the matrix or environment. The formation of free Fe^{+++} in aqueous environment of Ca^{++} , HCO_3^- , and Fe_2O_3 is an impossible relationship at surface conditions.



$$G_R = (+)62.15 \text{ Kcal/mole.}$$

The gastropod pellets and fragments that exhibited rimming by Fe_2O_3 , in most cases, had not been subjected to recrystallization. Therefore, it is possible that the recrystallization mechanism is either halted or slowed down by the armoring effect of Fe_2O_3 . It would seem significant to note in other sequences of carbonate rocks the relationship between Fe_2O_3 content and degree of recrystallization.

The other occurrences of ferric iron in carbonates are those most commonly noted in the form of stains and local distributions of Fe_2O_3 formed as a result of ground water alteration and/or surface weathering phenomena.

The X-ray diffraction studies indicated that pure Fe or Mn minerals are not present, hence these elements occur in solid solution with Ca and/or Mg in the carbonate matrix or in the insoluble clay fraction. The clay mineralogy of the Eiss Limestone suggests the presence of Fe^{++} in the chlorite minerals and the presence of Mn^{++} is also to be expected in the clays. The upper Eiss Limestone (Fig. 16) was found to contain more Mn and less Fe while the lower limestone contained more Fe and less Mn. These relationships can again be attributed to the clay fraction which

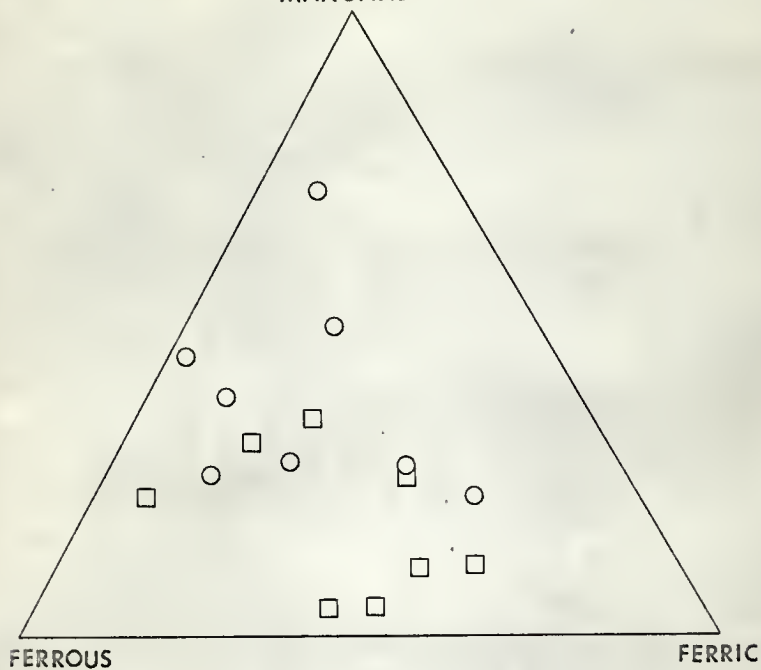
EXPLANATION OF FIGURE 16

Tertiary diagram for ferrous, ferric iron and manganese for the Eiss Limestone. Values for each cation calculated on the basis of 100 per cent.

☐ Lower Eiss Limestone

☐ Upper Eiss Limestone

FIGURE 16
MANGANESE



FERROUS IRON vs. FERRIC IRON vs. MANGANESE FOR EISS LIMESTONE

would have higher Fe^{++} values in proportion to the amount of insoluble residue. It does appear that the two limestones can be differentiated on the basis of their Mn and Fe contents.

It was also noted (Fig. 17) that in plotting % Mn vs. % Ca that a clear separation of upper and lower Eiss Limestone could be achieved which again is a reflection of the higher Mn content of the upper Eiss Limestone and the lower Mn content of the lower Eiss Limestone.

It is also interesting to note that as the Mn content increases, the Ca content decreases in both the upper and lower Eiss Limestones. This relation is possibly the result of undissolved Mn oxides in the insoluble residue as the per cent of insolubles present is inversely proportional to the per cent calcium. Another explanation is that Mn serves as an indicator of pH conditions in relation to CaCO_3 precipitation. For instance, an increase in pH (at the same Eh) would cause the precipitation of CaCO_3 but could decrease the Mn percentage so that slight fluctuation in the Mn content would be reflected in larger and opposite fluctuation in the amount of CaCO_3 precipitated.

According to the characteristic Mn values of Ronov and Ermishkina (1959) for arid and humid climates it would appear that the lower Eiss Limestone was deposited in a humid environment while the upper Eiss Limestone was deposited in a less humid to arid environment. The greater humidity of the lower Eiss climate could explain the greater amount of terrigenous influx at this

EXPLANATION OF FIGURE 17

Per cent manganese plotted against calcium for the Eiss Limestone. Note the inverse relationship between the fluctuations of each cation.

□ Lower Eiss Limestone

○ Upper Eiss Limestone

FIGURE 17



time. Heavy rains and swollen rivers would benefit rapid sedimentation in a humid climate.

The lower Eiss Limestone is closely associated with the average Mn content of sedimentary carbonates (530 ppm) but the upper Eiss Limestone shows values somewhat below this average. The latter could possibly be explained by recrystallization mechanisms, but no definite trends have been found.

SILICON GEOCHEMISTRY

The presence of silicon in carbonate rocks can be attributed to several sources:

- (1) detrital silicon (quartz, chert, etc.)
- (2) Si in terrigenous silicates (clay minerals, heavy, minerals, etc.)
- (3) authigenic silica in either matrix or fossil replacement of consolidated carbonates.

For these and several reasons the silicon geochemistry of carbonates is very complex; and even through a whole rock examination, such as performed on the Eiss Limestone, very little can be said concerning its geochemical significance. A boundary of 11.5% insoluble residuc and 8.5% silicon can be established, then differentiating the upper from the lower Eiss Limestone (Fig. 18).

In the northern sections of the lower Eiss Limestone the presence of terrigenous quartz silt was noted in thin section. This trend can be observed (Fig. 18) in the high SiO_2 content of samples 1086a, 1086b, 1087a, and 1087b. The latter samples are characteristically higher in total SiO_2 than any of the others - due to a high percentage of quartz silt. Hence, the lower Eiss unit's higher silica and insoluble percentages are only a reflection of increased clay mineral, detrital quartz, authigenic quartz, and heavy mineral silicate percentages.

There appears to be no definite trend in the silicon content of the upper Eiss unit. This could be due to local concentrations of silicon with varying replacement within the unit. It is also

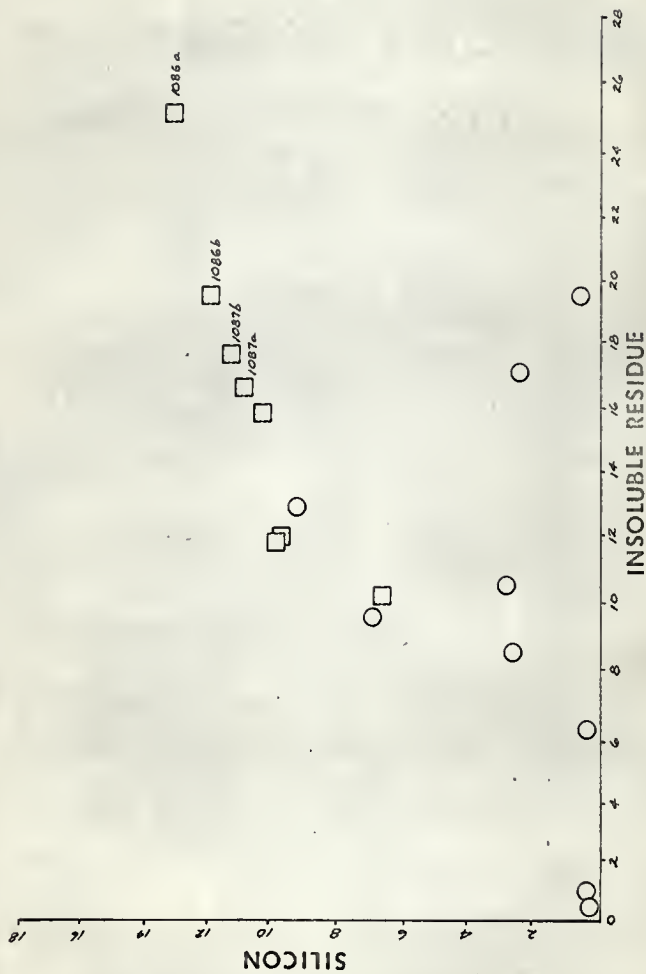
EXPLANATION OF FIGURE 18

Per cent insoluble residue plotted against per cent silicon for the Eiss Limestone. Note that the two limestones of the Eiss can be differentiated on the basis of each element.

□ Lower Eiss Limestone

○ Upper Eiss Limestone

FIGURE 18



noted that more solution effects are present in the upper Eiss unit which could locally mask the silicon content and also produce a lower total silicon content by preferential removal.

BULK CHEMISTRY

The bulk chemistry of the Eiss Limestone of Kansas (Tables 11 and 12) reflects the characteristics of an average shallow water limestone.

All of the Eiss Limestone sections correlated quite well using either channel samples (No. 1082) or grab samples (Nos. 1091-1093). It was noted, however, that certain variations in the bulk chemistry, such as silicon, would not have been detected unless closely spaced samples were collected. Therefore, it is the personal opinion of the writer that only closely spaced vertical samples will give the geochemist the control necessary for area correlation. Lateral sampling can be more widely separated due to relatively little change in the lateral direction as opposed to the vertical for the same distance.

The values of the specific oxides have very little meaning unless coupled with environmental information obtained from a petrographic analysis. Previous attempts at limestone geochemistry have failed due to a lack in petrographic control. For the environmental geochemist a tabulation of oxides with no petrography offers little assistance in the understanding of past environments. For this reason the writer has attempted to correlate geochemical variations with their petrographic equivalents in the previous sections.

TABLE 11

Major and minor element oxide conversions for
the Eiss Limestone. Total of each complete
oxide analysis is within laboratory error.

Table 11

Oxide Analyses of the Eiss Limestone of Kansas

	Sample No.	CaO	CO ₂	SiO ₂	MgO	FeO	Fe ₂ O ₃	StO	MnO	Oxide Sum
West Dam	1082 upper	53.51	41.99	0.90	1.12	0.18	0.51	0.023	0.041	98.27
	1084	45.06	35.38	9.54	4.02	0.21	0.31	0.020	0.051	94.59
	1086b lower	40.13	31.50	25.60	1.10	0.29	1.12	0.026	0.073	99.84
	1086a	36.85	28.95	28.00	2.89	0.40	1.69	0.027	0.074	98.68
East Spillway	1083 upper	47.85	37.54	5.55	0.66	0.20	0.28	0.019	0.042	92.14
	1087b lower	41.95	33.00	24.20	0.78	0.34	1.16	0.027	0.048	101.51
	1087a	42.24	32.08	23.60	2.51	0.35	2.05	0.022	0.073	102.93
Allendorph	1088a upper	51.49	40.40	1.22	0.83	0.26	0.20	0.037	0.042	94.48
	1088b	50.70	39.82	0.89	0.75	0.17	0.98	0.053	0.047	93.41
	1089	47.88	37.62	20.00	0.75	0.18	0.71	0.048	0.049	107.24
	1090 lower	47.67	37.41	22.04	0.84	0.34	0.86	0.030	0.042	109.23
Deep Creek	1091 upper	53.51	41.99	0.54	0.70	0.18	0.003	0.025	0.041	96.99
	1092	50.00	39.27	5.99	0.73	0.13	0.23	0.021	0.043	96.41
	1093	50.91	39.96	14.96	0.75	0.28	0.18	0.022	0.058	107.12
	1094 lower	46.37	36.40	21.36	0.79	0.31	0.34	0.024	0.061	105.66
	1095	49.35	38.73	14.42	0.79	0.25	0.45	0.024	0.060	104.08
Strong City	1097 upper	56.89	44.63	0.52	0.53	0.11	0.09	0.129	0.060	102.96
	1098 lower	47.93	37.63	18.60	0.47	0.45	0.17	0.038	0.062	105.35

TABLE 12

Bulk chemical variations in the Eiss Limestone.
Note major and minor element abundances variance
between the two limestones.

Table 12

Chemical Relationships in the Eiss Limestone Member

Sample No. & Location	Si%	Ca%	Mg%	Ca/Mg	Sr%	Sr/Ca 10 ³	E Fe	Fe ² %	Fe ³ %	Mn%	Mn/E Fe
1082 West Dam	0.42	38.24	0.80	47.92	0.0197	0.51	0.50	0.14	0.036	0.032	0.152
1084	4.46	32.19	2.88	11.19	0.0175	0.54	0.98	0.16	0.82	0.040	0.041
1086b	11.97	28.66	0.784	36.56	0.0225	0.83	1.10	0.241	0.86	0.056	0.051
1086a	13.09	26.32	1.93	13.67	0.0231	0.87	1.63	0.33	1.30	0.058	0.035
1083 East Spillway	2.59	34.20	0.47	72.75	0.0167	0.48	0.38	0.16	0.22	0.032	0.084
1087b	11.31	29.96	0.56	53.88	0.0204	0.68	1.17	0.28	0.89	0.037	0.032
1087a	11.03	30.17	1.80	16.76	0.0187	0.61	1.86	0.29	1.58	0.059	0.032
1091 Deep Creek	0.25	38.24	0.50	76.49	0.0215	0.56	0.15	0.148	0.002	0.031	0.207
1092	2.80	35.74	0.53	67.94	0.0181	0.50	0.28	0.11	0.17	0.034	0.121
1093	6.99	36.39	0.54	67.63	0.0190	0.52	0.37	0.23	0.14	0.045	0.122
1094	9.98	33.14	0.56	58.96	0.0208	0.62	0.52	0.26	0.26	0.047	0.090
1095	6.74	35.27	0.56	62.76	0.0208	0.58	0.55	0.20	0.35	0.046	0.084
1088a Allendorph	0.57	36.80	0.59	62.16	0.0323	0.87	0.37	0.21	0.16	0.033	0.089
1088b	0.42	36.22	0.54	67.32	0.0460	1.27	0.89	0.14	0.75	0.037	0.042
1089	9.35	34.20	0.54	63.57	0.0417	1.21	0.69	0.15	0.54	0.037	0.054
1090	10.30	34.07	0.60	56.78	0.0257	0.75	0.94	0.28	0.66	0.0330	0.035
1097 Strong City	0.24	40.66	0.38	107.56	0.1120	2.75	0.16	0.09	0.07	0.046	0.288
1098	9.86	34.25	0.34	101.34	0.0332	0.97	0.50	0.37	0.13	0.048	0.096

ENVIRONMENT OF DEPOSITION

Discussion

The Eiss Limestone Member of the Bader Limestone Formation was deposited in Wolfcampian time in shallow marine waters which covered a wide, very flat, shelflike basin in Kansas, Oklahoma and Nebraska. Lowlands bordered this Wolfcampian sea on the north, south and possibly the east. Tectonically active areas in southern Oklahoma supplied clastics which were spread northward by the gentle currents of the Eiss seas (Plate VII). These sediments mingled with those from the north and east thus creating a mixed representation of the several source areas. The climate was quite humid in lower Eiss Limestone times but by upper Eiss Limestone times the climate was essentially arid.

During lower Eiss Limestone time the sea shallowed until the northern, eastern and southern shorelines were comparatively near the area of investigation. At the same time the climate was quite moist supplying large quantities of terrigenous material and in some instances restricting fauna. The faunal distribution and clay mineral separations indicate a change in the bottom conditions at the Allendorph locality. Minor local uplifts could have occurred along the Nemaha Anticline, causing shoals in Allendorph locality during lower Eiss time with the uplift intensity increasing during upper Eiss time.

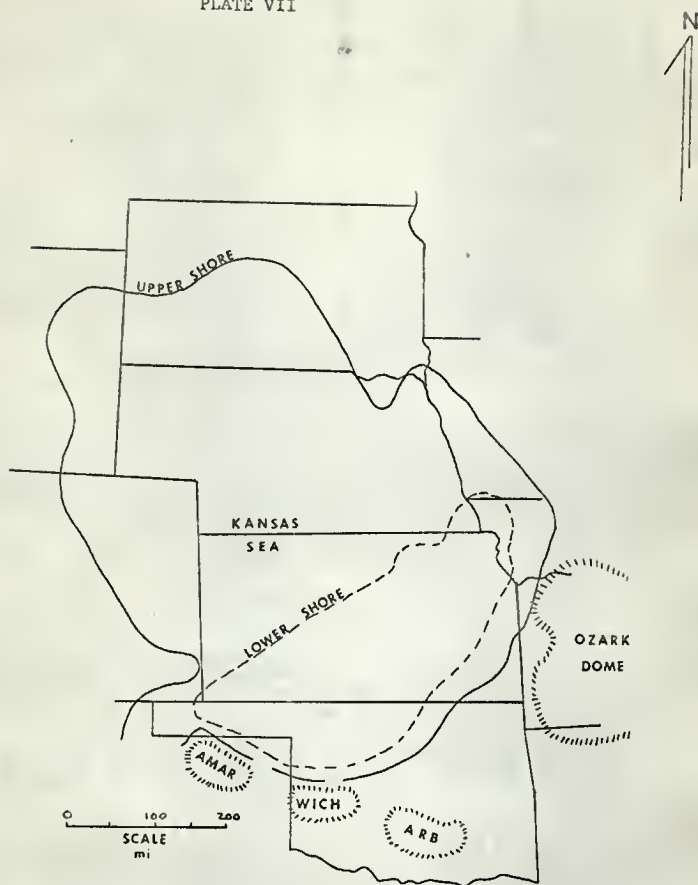
The salinity of the seas during lower Eiss time was probably more hypersaline than that for the upper Eiss time. The presence

EXPLANATION OF PLATE VII

Paleogeography during deposition of the Eiss Limestone
modified from Elias (1964).

Morphology of the basin was controlled by the local
tectonics and rates of basin subsidence. The basin
morphology was directly responsible for the developed Eiss
faunal facies.

PLATE VII



PALEOGEOGRAPHY OF THE EISS SEA
(after Elias, 1964)

of a shallower environment combined with a high terrigenous influx points to hypersaline conditions. Geochemically the higher concentrations of total iron and manganese in the lower unit could reflect a very restricted environment with basinal evaporation and concentration conditions.

During upper Eiss times the same environmental conditions persisted with a few exceptions. The presence of non-encrusting algae, a higher brachiopod fauna, less insoluble residue, less total iron and manganese would extend the upper Eiss Limestone into slightly deeper water with less restricted conditions. The definite shoal characteristics observed at the Allendorph locality in the upper Eiss Limestone again point to the effect of local uplifts or variations in bottom topography.

CONCLUSIONS

Through a combined investigation of carbonate petrography and geochemistry, the Eiss Limestone Member of Kansas was successfully subdivided and correlated. The depositional history of the Eiss Limestone with possibilities of source, basin type, and environment of deposition was studied in detail.

As a result of the petrographic investigation, the following conclusions characterize the Eiss Limestone:

- (1) The Eiss Limestone can be divided into two distinct limestones which include an upper porous, light-tan, less fossiliferous limestone unit and a lower argillaceous, light gray, more fossiliferous limestone unit.
- (2) Both units are characterized by an algal, shelly (molluse, pelecypod, brachiopod, gastropod) fauna and best fit the mollusean-mixed type of a typical eurythermic phase.
- (3) Due to some fragmentation and mixed fauna in a few sections the possibility of a mixed biocoenosis-thanatocoenosis faunal assemblage is suggested.
- (4) The upper Eiss unit was deposited in deeper water than the lower unit.
- (5) A more humid climate and hypersaline environment is postulated for the lower Eiss Limestone.
- (6) Conditions north and south of the Allendorph locality reflect changes which indicate a shoal or shallowing at the latter locality.

- (7) Both units are characterized by a high per cent of microspar which indicates recrystallization of the limestones.

The geochemical investigation of the Eiss Limestone correlates quite well with the petrographic evidence. In summary the following geochemical variations characterize the Eiss Limestone:

- (1) The Eiss Limestone Member can be divided into two distinct limestones based on differences in per cent calcium, silicon, total iron, ferrous iron, ferric iron, and manganese.
- (2) Lateral geochemical variations of cations can be used to correlate one section with another.
- (3) A biochemical as well as a chemical formation of the limestone units is postulated due to the presence of calcareous algae.
- (4) A slightly lower Ca/Mg ratio in the upper limestone unit could be indicative of deposition in deeper water and at a greater distance from shore.
- (5) The close similarity of Ca/Mg ratios within both units indicates a similarity in both relative depth and distance from shore, with occasional lateral fluctuations.
- (6) Both units have a low dolomite content (dolomite was noted in only five samples) which explains the overall low Mg content.
- (7) Magnesium alone cannot be used effectively as an environmental indicator due to its presence in clay minerals and possibly in heavy minerals.

- (8) Strontium in the Eiss Limestone is restricted to structural sites in the carbonate matrix and is not concentrated in celestite or other secondary minerals.
- (9) The data, except from one location (Upper Eiss-Strong City), indicate a loss of strontium as a result of recrystallization. The average of 16 samples is 220 ppm.
- (10) The Upper Strong City section which shows little petrographic evidence of recrystallization, has a strontium value of 1120 ppm, which indicates little or no loss of strontium.
- (11) It may be possible to use strontium as an index of the degree of recrystallization of limestones.
- (12) Strontium values increase to the south rapidly, which could be indicative of a shore in that direction.
- (13) The average $\text{Sr}^{87}/\text{Sr}^{86}$ initial ratio for the Eiss Limestone Member is 0.7081 ± 0.001 which fits well the marine geochron for other Permian isotopic data.
- (14) Ferrous iron values below 0.22 per cent are characteristic of the upper unit while values greater are indicative of the lower unit.
- (15) Some primary ferric iron exists in the Eiss Limestone as shown by iron armoring on pellets.
- (16) Ferrous iron and manganese exist in solid solution with calcium and/or magnesium either in the matrix or in the insoluble fraction, but not in minerals where they are the dominant cation.

- (17) The upper unit contains more Mn and less Fe^{++} than the lower unit, which again can be correlated with the insoluble fraction.
- (18) Mn increases to the south in the lower unit which could indicate a shore or reef where Mn was directly precipitated by algae.
- (19) As the Mn content increases the Ca content decreases in both limestone units. This relationship could result from the deposition of insolubles or a pH change.
- (20) The upper Eiss Limestone was deposited under arid conditions while the lower Eiss Limestone was deposited under humid conditions as indicated by the range of Mn values for each.
- (21) Recrystallization may have possibly affected the Mn concentrations in each unit.
- (22) Silicon reflects the terrigenous influx and post-depositional effects with correlative geochemical relationships possible to some degree.

FINAL CONCLUSION

The application of X-ray diffraction and spectroscopy, atomic absorption techniques, mass spectroscopy, and wet chemical methods to the study of limestones combined with carbonate petrography correlate quite well. Although petrographic or geochemical investigations can be made separately, the combined usefulness of each should be of great future value to the carbonate investigator. It is only when both are taken into consideration that implication can become fact.

ACKNOWLEDGMENTS

The writer would like to offer his thanks and appreciation to Dr. D. C. Brookins, the author's major professor, for his aid and assistance during the investigation and especially for his work with the mass spectrometer. I would also like to thank Kansas State University for the research assistantship which made this thesis possible.

Thanks go to Dr. J. R. Chclikowsky, Dr. Claude Shenkel, and Dr. F. C. Lanning for their comments and criticisms concerning this thesis.

Special thanks are also due to the others who assisted the writer in various fields: to Dr. Sam Chaudhuri for his help with the clay mineralogy, to the State Geological Survey of Kansas for the use of chemical standards, to the Chemistry Department at Kansas State University for the use of their equipment, to the Kansas State Highway Department for their advise in the field, and to Shell Oil Company, Midland, Texas, for their assistance in preparing the manuscript copies.

APPENDIX

INSOLUBLE RESIDUE

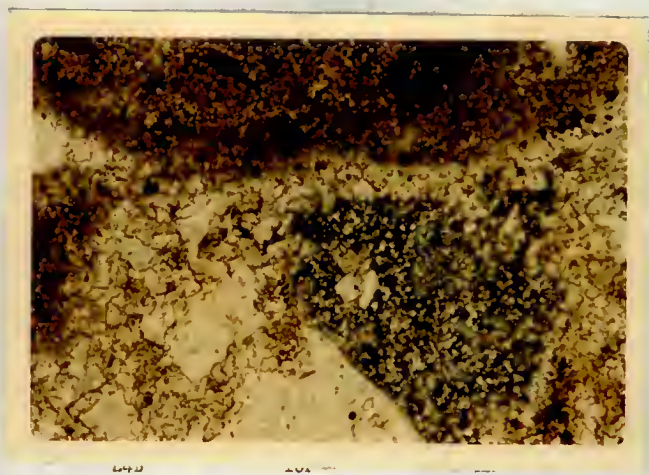
SAMPLE NO.	LOCATION	WEIGHT PER CENT
1086b	West Dam	19.44 (grams)
1086a		25.65
1083	East Spillway	8.50
1087b		17.50
1087a		16.55
1088a	Allendorph	19.36
1088b		6.03
1089		12.87
1090		15.80
1091	Deep Creek	1.00
1092		10.48
1093		9.57
1094		11.78
1095		10.30
1097	Strong City	0.59
1098		11.92

CLAY MINERALS

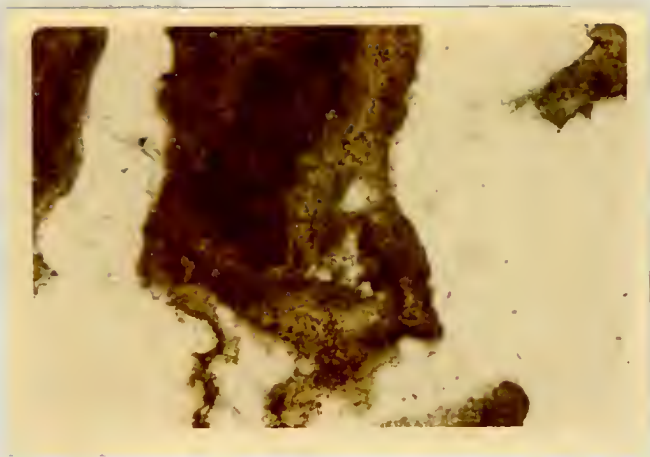
LOCATION	SAMPLE NO.	CLAY MINERAL(S)
West Dam	1082	Illite Chlorite
	1084 upper	Illite Montmorillonite Mixed-layer
West Dam	1086b lower	Illite Montmorillonite Mixed-layer
	1086a	Illite Montmorillonite Mixed-layer Vermiculite
East Spillway	1083	Illite Montmorillonite Mixed-layer
	upper	
East Spillway	1087b lower	Illite Montmorillonite Mixed-layer
	1087a	Illite Montmorillonite Mixed-layer
Deep Creek	1091	Illite
	1092	Illite
	1093 upper	Illite
Deep Creek	1094 lower	Illite Montmorillonite
	1095	Illite Montmorillonite Mixed-layer

CLAY MINERALS

LOCATION	SAMPLE NO.	CLAY MINERAL(S)
Allendorph	1088a	Illite Chlorite
	1088b	Illite
	1089	Illite Montmorillonite Mixed-layer Vermiculite
	upper	
Allendorph	1090	Illite Vermiculite Montmorillonite
	lower	
Strong City	1097	upper Illite
Strong City	1098	lower Chlorite Mixed-layer



Burrow filled with sparry calcite. Adjacent walls have been
recrystallized.

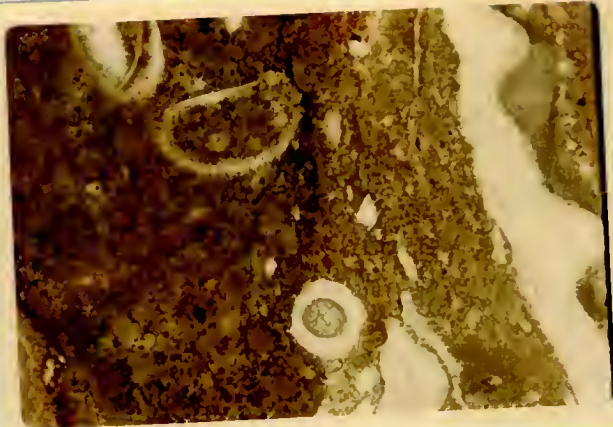


E2D

10P

XN

Recrystallized Anchicodium (ghosts) micrite. Complete
recrystallization.

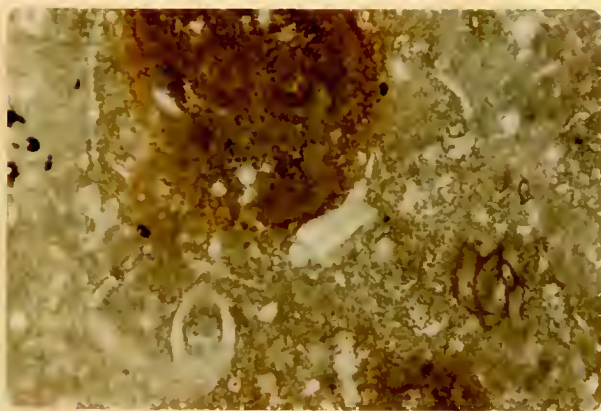


E2A

10P

PPL

Pellet containing brachiopod spine and ostracod valves. Note
ferric oxide rimming of pellet.

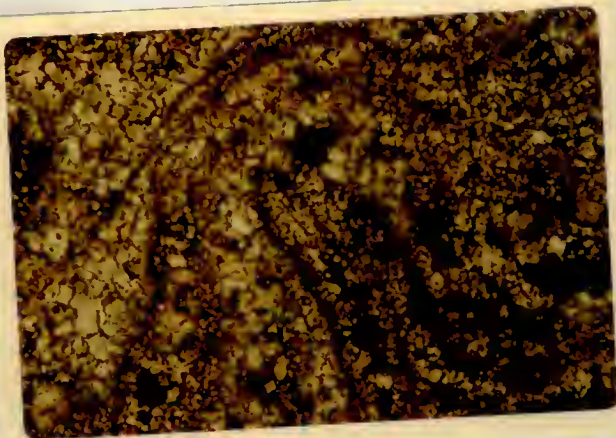


E2A

10P

PPL

Ferric oxide pellet surrounded by recrystallized micrite. Note
lack of recrystallization within pellet.

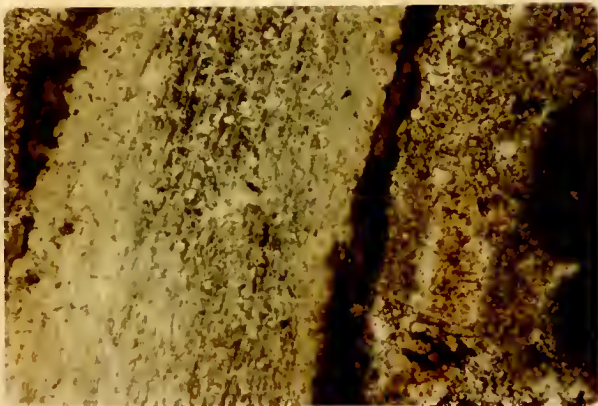


SC-1

10P

PPL

Algal dismicrite formed by either burrowing organisms or areal disturbances (i.e. storms, etc.)



ED-4

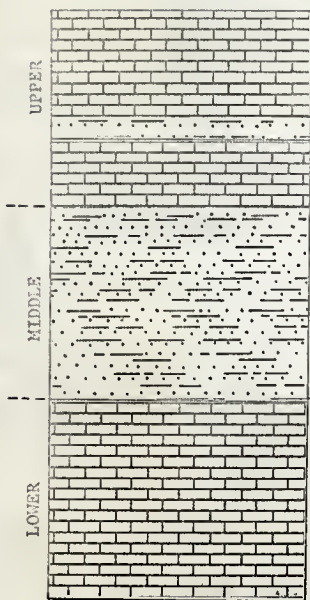
10P

XN

Algal (Osagia) coated brachiopod in the algal bryozoan facies.

SECTION E-1

TUTTLE CREEK WEST DAM



Gray to tan very dense limestone.
Relatively unfossiliferous. Limonite
stains on fresh samples.

Shale break which lenses out locally.

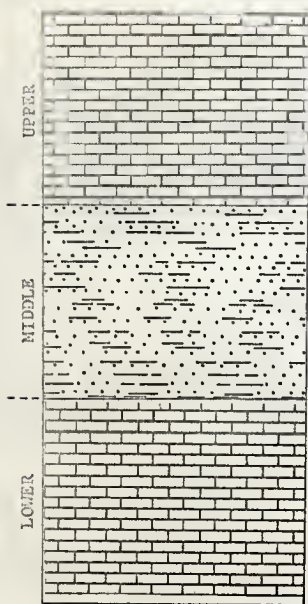
Gray, soft, shaley limestone. Weathers
to a yellow clay. Average fossil
content.

Gray to black limey shale.

Gray shaley limestone. Profuse fossils
with bryozoan fragments abundant.
More dense at bottom than at top.
Grades into overlying middle shale unit.

SECTION E-2

TUTTLE CREEK EAST SPILLWAY



Massive gray to tan very dense limestone. Sparse fossil content. Frequent limonite stains on joints and fractures.

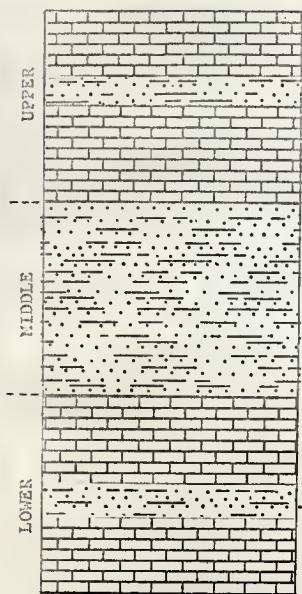
Lower 0.6ft. soft clayey limestone. Definite break between upper and middle units.

Gray to black limey shale.

Gray shaley limestone. Very fossiliferous with bryozoans and molluscs abundant. Fissility developed at top of limestone which grades into middle shale unit.

SECTION E-3

DEEP CREEK



Tan dense limestone with very pitted surface; sparsely fossiliferous.
Shale break.

Shale break.

Tan dense limestone with few fossils.
Sharp contact with middle shale.

Tan limey shale.

Black limey shale.

Tan limey shale.

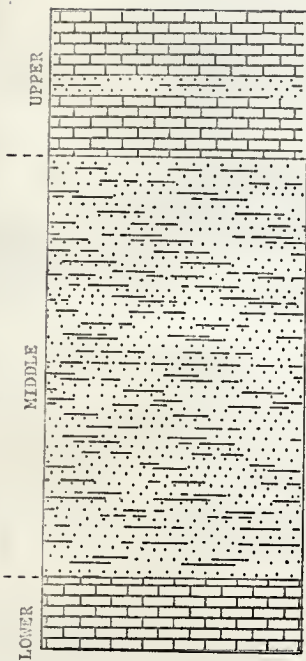
Gray shaley limestone with abundant fossils. Molluscs well represented.
Great fissility at top of unit.

Shale break.

Gray shaley limestone but more dense than that above shale break. Fossils abundant.

SECTION E-4

ALLENDORPH



Purple to gray dense limestone. Very solutioned surface. Sparsely fossiliferous but with some molluscs.

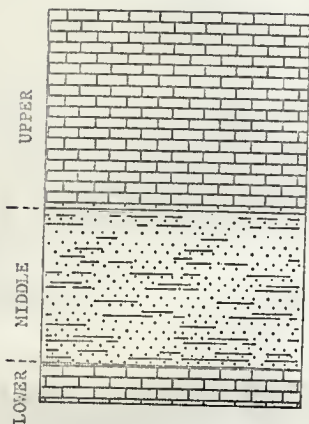
Shale break with high pelecypod content. Tan to gray less dense limestone with abundant shelly fauna.

Vericolored shale; some quite limey.

Gray shaley limestone with average fossil content. Shelly fauna visible. Sharp contact with middle shale.

SECTION E-5

STRONG CITY



Very dense tan-gray limestone with deeply solutioned surface. Relatively unfossiliferous and containing vugs with calcite fillings.

Tan, slightly limey shale.

Tan, soft, shaley limestone with sparse fossil content and gradational break to middle shale.

REFERENCES

- Archie, G. E., 1952, Classification of carbonate reservoir rocks and petrophysical considerations: Am. Assoc. Petroleum Geologists Bull., v. 36, no. 2, p. 278-297.
- Bass Becking, L. G. M., Kaplan, I. R., and Moore, D., 1960, Limits of the natural environment in terms of pH and oxidation-reduction potential: Jour. Geol., v. 68, p. 243-284.
- Bisque, R. E., and Lemish, J., 1959, Insoluble residue-magnesium content relationship of carbonate rocks from the Devonian Cedar Valley Formation: Jour. Sed. Petrology, v. 29, no. 1, p. 73-76.
- Brookins, D. G., 1966, Strontium isotopic variations in carbonate rocks from Riley County, Kansas: Mass. Inst. Tech. Fourteenth Annual Report, p. 159.
- Chave, K. E., 1952, A solid solution between calcite and dolomite: Jour. Geol., v. 60, p. 190-192.
- 1954b, Aspects of the biogeochemistry of magnesium-2: calcareous sediments and rocks: Jour. Geol., v. 62, p. 587-599.
- 1954a, Aspects of the biogeochemistry of magnesium: 1. Calcareous marine organisms: Jour. Geol., v. 62, p. 266-283.
- Chilingar, G. V., 1956, Relationship between Ca/Mg ratio and geologic age: Am. Assoc. Petroleum Geologists Bull., v. 40, p. 2256-66.
- 1957, Classification of limestones and dolomites on the basis of Ca/Mg ratio: Jour. Sed. Petrology, v. 27, p. 187-189.
- 1960, Ca/Mg ratio of calcareous sediments as a function of depth and distance from shore: Compass, v. 37, no. 3, p. 182-86.
- 1962, Possible loss of magnesium from fossils to the surrounding environment: Jour. Sed. Petrology, v. 32, p. 136-39.
- 1963, Ca/Mg and Sr/Ca ratios of calcareous sediments as a function of depth and distance from shore: Jour. Sed. Petrology, v. 33, no. 1, p. 236.

- Condra, G. E., 1927, The stratigraphy of the Pennsylvanian system in Nebraska: Neb. Geol. Survey Bull. 1, ser. 2, p. 16.
- 1935, Geologic cross section, Forest City, Missouri, to Du Bois, Nebraska: Neb. Geol. Survey Paper 8.
- Degens, E. T., 1965, Geochemistry of sediments: Prentice-Hall, New Jersey, p. 98-141.
- , and Epstein, S., 1964, Oxygen and carbon isotope ratios in coexisting calcites and dolomites from recent and ancient sediments: *Geochim et Cosmochim Acta*, v. 28, p. 23-44.
- Dietrich, H. A., 1956, Paleogeology of the shale in the Eiss Limestone (Lower Permian) in Chase County, Kansas: Kans. Univ. M. S. Thesis, p. 42-48.
- Elias, M. K., 1937, Depth of deposition of the Big Blue (late Paleozoic) sediments in Kansas: *Geol. Sec. American Bull.*, v. 48, p. 403-432.
- 1964, Depth of late Paleozoic sea in Kansas and its megacyclic sedimentation, in Symposium on cyclic sedimentation: *Kans. Geol. Survey Bull.*, v. 169, p. 97.
- Emery, K. O., Tracey, J. I., and Ladd, H. S., 1954, Geology of Bikini and nearby atolls: U. S. Geol. Survey Prof. Paper 260-A, Pt. 1-Geology, p. 236.
- Fairbridge, R. W., 1957, The dolomite question in Regional aspects of carbonate deposition: *S.E.P.M.*, Special Publ. 5, p. 125-178.
- Faure, G., Hurley, P. M., and Powell, J. L., 1965, The isotopic composition of strontium in surface water from the North Atlantic Ocean: *Geochim. et Cosmochim. Acta*, v. 29, p. 209-220.
- Folk, R. L., 1964, Petrology of sedimentary rocks: University of Texas laboratory manual, Hemphill's, Austin, Texas, p. 141-159.
- Friedman, G. M., 1959, Identification of carbonate minerals by staining methods: *Jour. Sed. Petrology*, v. 29, no. 1, p. 87-97.
- 1964, Early diagenesis and lithification in carbonate sediments: *Jour. Sed. Petrology*, v. 34, p. 777-813.

Carrels, R. M. and Christ, C. L., 1965, Solutions, minerals and equilibria: New York, Harper and Row, p. 209, 242.

Gast, P. W., 1960, Limitations on the composition of the upper mantle: Jour. Geophys. Res., v. 65, p. 1287-1297.

Coldberg, E. D., 1957, Biogeochemistry of tract metals: Geol. Soc. America Mem. 67, p. 345-57.

Coldsmith, J. R., 1959, Some aspects of the geochemistry of carbonates, in Researches in geochemistry: New York, John Wiley and Sons, Inc., p. 336-368.

Crabau, A. W., 1904, Paleozoic coral reefs: Geol. Soc. America Bull., v. 14, p. 337-352.

Graf, D. L., Blyth, C. R., and Stemmler, R. S., 1955, Dolomite-magnesium calcite relations at elevated temperatures and carbon dioxide pressures: Geochim. et Cosmochim. Acta, v. 7, p. 109-128.

-----, and Lamar, J. E., 1955, Properties of calcium and magnesium carbonates and their bearing on some uses of carbonate rocks: Econ. Geology 50th Anniv. Vol., p. 639-713.

(X) ----- 1960, Geochemistry of carbonate sediments and sedimentary carbonate rocks-Pt. 3 Minor element distribution: Illinois State Geol. Survey, Circular 297, p. 25-26, 32-37.

Grim, R. E., 1953, Clay mineralogy: New York, McCraw-Hill, p. 384.

Hedge, C. E. and Walthall, F. G., 1963, Radiogenic strontium - 87 as an index of geologic processes: Science, v. 140, p. 1214-1217.

Herzog, L. F., Pinson, H. W., and Cormier, R. F., 1958, Sediment age determination by Rb/Sr analysis of glauconite: Amer. Assoc. Petroleum Geologists Bull., v. 42, p. 717-733.

X Hewett, D. F., 1933, Manganese in sediments, in Treatise on sedimentation: New York, Dover Publications, p. 562-81.

Hirst, D. M., 1962, The geochemistry of modern sediments from the Gulf of Paria-I: Geochim. et Cosmochim. Acta, v. 26, p. 309-335.

(V) Horn, M. K., and Adams, J. A. S., 1966, Computer-derived geochemical balances and element abundances: Geochim. et Cosmochim. Acta., v. 30, p. 279-97.

- Huber, N. K., 1958, The environmental control of sedimentary iron minerals: *Econ. Geol.*, v. 53, p. 123-40.
- Illing, L. V., 1954, Bahaman calcareous sands: *Am. Assoc. Petroleum Geologists Bull.*, v. 38, p. 1-95.
- ✓ Ingerson, E., 1962, Problems of the geochemistry of sedimentary carbonate rocks: *Geochim. et Cosmochim. Acta*, v. 26, p. 815-849.
- Jewett, J. M., 1959, Graphic column and classification of rocks in Kansas: *Kans. Geol. Survey*, in preparation.
- Kahle, C. F., 1965, Possible roles of clay minerals in the formation of dolomite: *Jour. Sed. Petrology*, v. 35, no. 2, p. 448-453.
- ✓ Keith, M. L., and Degens, E. T., 1959, Geochemical indicators of marine and freshwater sediments in *Researches in geochemistry*: New York, John Wiley and Sons, Inc., p. 38-61.
- Krauskopf, K. B., 1957, Separation of magnesium from iron in sedimentary processes: *Geochim. et Cosmochim. Acta*, v. 12, p. 61-84.
- Kulp, J. L., Turekian, K., and Boyd, D. W., 1952, Sr content of limestones and fossils: *Geol. Sec. American Bull.*, v. 63, p. 701-716.
- Lane, N. G., 1964, Paleoeecology of the Council Grove Group (Lower Permian) in Kansas, based upon microfossil assemblages: *Kans. Geol. Survey Bull.*, v. 170, pt. 5, 28 p.
- Laning, F., 1967, Department of Chemistry, Kans. St. Univ., personal communication.
- Lowenstam, H. A., 1953, Environmental relations of modification compositions of certain carbonate secreting marine invertebrates: *Nat. Acad. Sci. Proc.*, v. 40, p. 39-48.
- McCrone, A. W., 1964, Paleoeecology and biostratigraphy of the Red Eagle Cyclothem (Lower Permian) in Kansas: *Kans. Geol. Survey Bull.*, v. 164, p. 68-70.
- Mudge, M. R., 1949, The Pre-Quaternary stratigraphy of Riley County, Kansas: *Kans. St. Univ. M.S. Thesis*, 187 p.
- , and Crumpton, C., 1959, Geology of Wabaunsee County, Kansas: *U. S. Geol. Survey Bull.* 1068.

- Mudge, M. R. and Yochelson, E. L., 1962, Stratigraphy and paleontology of the uppermost Pennsylvanian and lowermost Permian rocks in Kansas: U. S. Geol. Survey, Prof. Paper 323, 213 p.
- Murray, J. W., 1954, The deposition of calcite and aragonite in caves: Jour. Geol., v. 62, p. 481.
- Odum, H. T., (1950) Biogeochemistry of strontium: Yale University Ph. D. Thesis, p. 161.
- Pilkey, O. H., and Hower, J., 1960, The effect of environment on the concentration of skeletal magnesium and strontium in Dendroaster: Jour. Geol., v. 68, p. 203-216.
- Powell, J. L., Hurley, P. M., and Fairbairn, H. W., 1965, The strontium isotopic composition and origin of carbonates, in the carbonatites: New York, Wiley-Interscience, 280 p.
- Ronov, A. B. and Ermishkina, A. I., 1959, Distribution of manganese in sedimentary rocks: Geokhimiya, p. 206-225.
- Sass, E., 1965, Dolomite-calcite relationships in sea water: theoretical considerations and preliminary experimental results: Jour. Sed. Petrology, v. 35, p. 339-347.
- Siegel, F. R., 1961, Variations of Sr/Ca ratios and Mg contents in recent carbonate sediments of the northern Florida Keys area: Jour. Sed. Petrology, v. 31, p. 336-42.
- Smith, J. P., 1967, Petrology of Brite Ignimbrite, Trans Pecos, Texas: Kans. St. Univ. M.S. Thesis, 97 p.
- Stauffer, K. W., 1960, Quantitative petrographic study of Paleozoic carbonate rocks, Caballo Mountains, New Mexico: Stanford Univ. Ph. D. Thesis, p. 32-39.
- Steidtmann, E., 1917, Origin of dolomite as disclosed by strains and other methods: Geol. Sec. America Bull., v. 28, p. 431-450.
- Sternberg, T. E., Fischer, A. G., and Holland, H. O., 1959, Strontium content of calcites from the Steinplatte Reef Complex: Geol. Soc. America Bull., v. 70, p. 1681.
- Stindl, Heribert, 1966, Clay mineralogy of Cottonwood Limestone: Kans. St. Univ. M.S. Thesis, p. 66-73.
- Swinchatt, F. G., 1965, Shell mineralogy in Paleozoic invertebrates: Science, v. 132, p. 1031.

- Thompson, T. G. and Chow, T. J., 1956, The Sr/Ca atom ratio in carbonate secreting marine organisms: Papers in Marine Biology and Oceanography, Univ. Wash. Pub. 184, p. 20-39.
- Turckian, K., 1955, Paleoeological significance of the Sr/Ca ratio in fossils and sediments: Geol. Sec. America Bull., v. 66, p. 155-58.
- , and Kulp, J. L., 1956, The geochemistry of strontium: Geochim. et Cosmochim. Acta, v. 10, p. 245-296.
- Vinogradov, A. P., Ronov, A. B., and Ratynsky, V. M., 1952, Changes of chemical composition of carbonate rocks of the Russian platform: Akad. Nauk SSR Izv., Geol. Scr., no. 1, p. 33-50.
- , Ronov, A. B., and Ratynsky, V. M., 1957, Variations in the chemical composition of carbonate rocks of the Russian platform: Geochim. et Cosmochim. Acta, v. 12, p. 273-76.
- Zeller, E. J., and Wray, J. O., 1956, Factors influencing precipitation of calcium carbonate: Am. Assoc. Petroleum Geologists, v. 40, p. 140-152.
- Zen, E., 1960, Carbonate equilibria in the open ocean and their bearing on the interpretation of ancient carbonate rocks: Geochim. et Cosmochim. Acta, v. 18, p. 57-71.
- Zenger, D. H., 1965, Calcite-dolomite ratios vs. insoluble content in the Lockport Formation (Niagran) in New York State: Jour. Sed. Petrology, v. 35, no. 1, p. 262-64.

CARBONATE PETROGRAPHY AND GEOCHEMISTRY OF THE
EISS LIMESTONE OF KANSAS

by

PAUL L. DOWLING, JR.

B.S., Old Dominion College, 1965

AN ABSTRACT OF A MASTER'S THESIS

submitted in partial fulfillment of the

requirements for the degree

MASTER OF SCIENCE

Department of Geology and Geography

KANSAS STATE UNIVERSITY
Manhattan, Kansas

1967

ABSTRACT

The Eiss Limestone Member, Bader Limestone Formation, Council Grove Group of lower Permian Wolfcampian age has been investigated by geochemical and petrographic methods. Samples from outcrops in Riley, Geary, Pottawatomie, Wabaunsee, and Chase Counties were studied. This limestone can be traced along an outcrop belt from extreme southern Nebraska to northern Oklahoma. Although it varies considerably in thickness over its entire areal distribution, it is constantly present in the area of sampling for this study.

A combined geochemical and sedimentary petrographic study has been undertaken to test theories of geochemical correlation and of the depositional conditions of the Eiss Limestone. Further, the validity of geochemical data as an interpretive tool for the carbonate petrographer has been tested.

Petrographically the Eiss Limestone Member can be divided into two distinct limestones: an upper unit which was deposited in a shallow water marine environment, and a lower unit which was deposited in a shallower, more clayey, marine environment. A more apparent environmental differentiation can be made along strike within each unit. The upper unit is an algal shelly brachiopod facies (55 feet deep) to the north while in the south it grades into a shallower algal molluscan facies (30 feet deep). The lower unit is an algal bryozoan shelly facies (40 feet deep) to the north while in the south it grades into a slightly algal molluscan echinoderm facies (15 feet deep). Although the differences in

depth of sedimentation and faunal assemblages along strike are subtle, a general trend of a southerly source or shore direction is suggested.

Geochemical investigations show that the Eiss Limestone can be divided into two strikingly different limestones. The upper unit has characteristically higher Ca/Mg ratios, decreased ferrous iron content, and increased manganese content relative to the lower unit. Correlation is quite possible along strike using Ca/Mg ratios, Sr/Ca ratios, and total concentrations of ferrous iron, manganese, and strontium. The data further suggest a deeper formational environment for the upper unit. These implications support the petrographic data.

Strontium isotopic analyses yielded an average $\text{Sr}^{87}/\text{Sr}^{86}$ initial ratio for the Eiss Limestone of 0.7081 ± 0.001 which is consistent with other Permian isotopic data for a typical marine geochron.

It is clear that a thorough combination of carbonate petrography and geochemistry can be used effectively to support each other in an investigation of correlation and environment of deposition in alternating shale and limestone sequences.